

Part I. The proapoptotic C16-ceramide-dependent pathway requires the death-promoting factor Btf in colon adenocarcinoma cells

1. Summary

It is now recognized that ceramide exert a wide range of biological functions in relation to cellular signalling. The role of ceramide in the regulation of growth arrest, senescence, and/or apoptosis has received special attention (Saddoughi *et al.* 2008). In fact, apoptosis can often be induced in cancer cells by elevation of endogenous ceramide levels in response to a variety of apoptotic stimuli such as cytokines (IL-1), death receptor ligands (Fas ligand), heat stress, oxidative stress, chemotherapeutic agents, and ionizing or ultraviolet (UV) radiation (Pettus *et al.* 2002; Ogretmen and Hannun 2004; Lin *et al.* 2006; Hannun and Obeid 2008; Bartke and Hannun 2009). The use of exogenous cell-permeable short-chain ceramide particularly C2- and C6-ceramides could also promote apoptotic pathways in cancer cells (Dobrowsky and Hannun 1992; Dobrowsky *et al.* 1993; Obeid *et al.* 1993; Martin *et al.* 1995; Ogretmen and Hannun 2001; Fillet *et al.* 2003; Fillet *et al.* 2005). Several studies have attempted to further define the specific role of ceramide in cell death. However, the mechanisms by which ceramide mediates antiproliferative pathways or inhibits prosurvival effects are not yet well-defined (Lin *et al.* 2006). For all these reasons, we investigated the signalling pathways triggered by exogenous long chain ceramide, especially C16-ceramide.

We showed that C16-ceramide induced a decrease in viability of adenocarcinoma cells, partly due to apoptosis, as demonstrated by caspase-3 activation and poly (ADP-ribose) polymerase (PARP) cleavage. To find new proteins involved in the ceramide signalling pathway, we performed a two-dimensional differential in-gel electrophoresis (2D-DIGE). 51 proteins were found to be differentially expressed in C16-ceramide treated versus control HCT116 cells. These proteins are notably involved in cell proliferation, apoptosis, protein transport and transcriptional regulation. Among them, the cell death promoting factor Btf was, for the first time, found to be implicated in the apoptotic signal triggered by ceramide. Indeed, Btf-depleted colon cancer cells were found to be more resistant to death triggered by C16-ceramide. Downstream targets and mechanisms of Btf-induced apoptosis remain poorly understood. We discovered that the transfection of GFP-Btf expression plasmid up-regulated p53 and BAX protein levels whereas pBcl-2 and Mdm2 expression were down-regulated.

Results I

Moreover, we demonstrated that the cotransfection of MDM2-LUC plasmid and Btf siRNA induced a significant increase in luciferase activity of the MDM2 promoter after C16-ceramide treatment. All these results suggest that Btf plays an important role in the proapoptotic ceramide-dependent signalling pathway.

2. Article

The proapoptotic C16-ceramide–dependent pathway requires the death-promoting factor Btf in colon adenocarcinoma cells

Journal of Proteome Research

The Proapoptotic C16-ceramide-Dependent Pathway Requires the Death-Promoting Factor Btf in Colon Adenocarcinoma Cells

Anne-Françoise Rénert,[†] Pierre Leprince,[‡] Marc Dieu,[§] Jenny Renaud,^{||} Martine Raes,[§] Vincent Bours,[†] Jean-Paul Chapelle,[†] Jacques Piette,[†] Marie-Paule Merville,[†] and Marianne Fillet^{*†}

GIGA Signal Transduction, Units of Medical Chemistry and Genetics, University of Liège, Belgium, Sart-Tilman, Belgium, GIGA Neuroscience, University of Liège, Sart-Tilman, Belgium, Unité de Biochimie Cellulaire et Biologie, Spectrométrie de masse, Université de Namur, Belgium, and Department of Environment and Agrobiotechnologies, Centre de Recherche Public - Gabriel Lippmann, Belvaux, Luxembourg

Received June 16, 2009

Ceramides are central molecules in sphingolipid metabolism. They are involved in the regulation of cancer-cell growth, differentiation, senescence and apoptosis. To better understand how these secondary messengers induce their biological effects, adenocarcinoma cells (HCT116) were treated with exogenous long-chain ceramides (C16-ceramide) in order to mimic endogenous sphingolipids. This treatment induced a decrease of cell viability partly due to apoptosis as shown by PARP cleavage and a decrease of pro-caspase 3. Two-dimensional differential in-gel electrophoresis (2D-DIGE) revealed the differential expression of 51 proteins in response to C16-ceramide. These proteins are notably involved in cell proliferation, apoptosis, protein transport and transcriptional regulation. Among them, the cell death-promoting factor Btf was found to be implicated in the apoptotic signal triggered by ceramide. In adenocarcinoma cells, Btf regulates apoptosis related proteins such as Mdm2, p53, BAX and ⁹Bcl-2 and thus plays an important role in the ceramide mediated cell death. These findings bring new insight into the proapoptotic ceramide-dependent signaling pathway.

Keywords: 2D-DIGE • cancer cells • ceramide • Btf • apoptosis

Introduction

Apoptosis, or programmed cell death, plays an essential role in normal development and tissue homeostasis. Disruption of regulated apoptotic processes leads to various physiological abnormalities including cancer, autoimmune diseases, and neurodegenerative disorders.^{1–3} It is now recognized that ceramides exert a wide range of biological functions in relation to cellular signaling. The role of ceramides in the regulation of growth arrest, senescence, and/or apoptosis has received special attention.³ However, the mechanisms by which ceramide mediates antiproliferative pathways or inhibits pro-survival effects are not yet well-defined.⁴

Apoptosis can often be induced in cancer cells by elevation of endogenous ceramide levels in response to a variety of apoptotic stimuli such as Fas ligand, TNF- α , oxidative stress, chemotherapeutic agents, and ionizing or UV radiation.⁵ Ceramide can be produced in at least two distinct ways. It can be generated through the *de novo* synthesis mediated by serine-

palmitoyl transferase or through the hydrolysis of sphingomyelin.² The accumulation of ceramide can also be caused by small molecules like B13, an inhibitor of acid ceramidase (CDase).⁶ A number of downstream targets of ceramide have been identified including phosphatases and kinases, such as Akt, protein kinase C (PKC), kinase suppressor of Ras (KSR), MAP kinases, phospholipase D and the ceramide-activated protein phosphatases (CAPPs) including the serine/threonine protein phosphatases PP1 and PP2A.^{3,7}

Recently, Swanton et al. showed that down-regulation of a ceramide transport protein, CERT, sensitizes cancer cells to multiple cytotoxic agents, suggesting that the regulation of sphingolipid metabolism by CERT might confer a survival advantage to cancer cells.⁸

The use of ceramide analogues could also promote apoptotic pathways in cancer cells.^{3,9,10} Bielawska et al. observed that treatment with exogenous ceramides inhibited MCF7 cell growth.⁹ It should also be noted that treatment of cells with exogenous ceramides may result in the generation of endogenous long-chain ceramide via the sphingosine recycling pathway.³ Sultan et al. showed that this alternative pathway for the generation of endogenous long-chain ceramide in response to exogenous C6-ceramide is regulated by ROS and seems to be important for the regulation of c-Myc in A549 cells.¹⁰

* To whom correspondence should be addressed. M. Fillet, Laboratory of Medical Chemistry, GIGA-R, B34, University of Liège, Sart-Tilman, 4000 Liège, Belgium. Tel: 0032-4-3664354. Fax: 0032-4-3664347. E-mail: marianne.fillet@ulg.ac.be.

[†] GIGA Signal Transduction, Units of Medical Chemistry and Genetics, University of Liège.

[‡] GIGA Neuroscience, University of Liège.

[§] Université de Namur.

^{||} Centre de Recherche Public - Gabriel Lippmann.

Several studies have attempted to further define the specific role of ceramide in cell death. The tumor suppressor protein p53 and the Bcl-2 proteins family are key components of the tumor response to stress, and ceramide has been linked to each of these mediators.¹¹ In the absence of stress signals, the activity of p53 is regulated to allow normal cell proliferation and to maintain cell viability. Mdm2 (murine double minute) is crucial for this process. Indeed, Mdm2 inhibits p53 activity, giving rise to a negative feedback loop.¹² In response to cellular stress, such as DNA damage or oncogene activation, p53 is stabilized and modulates the transcription of target genes involved in cell-cycle control (i.e., *p21*), DNA repair and synthesis (i.e., *GADD45*) and apoptosis (i.e., *BAX*, *Puma*, and *Noxa*).¹³ Additionally, Mdm2 can function in a p53-independent manner. Indeed, Mdm2 overexpression suppresses *p21^{Cip1/Waf1}*-induced growth arrest in human p53^{-/-} and p53^{-/-}/Rb^{-/-} cells.^{14,15} In this study, p21 was found to be degraded by the proteasome independently of ubiquitination and p53/Rb status. Furthermore, another group demonstrated that Mdm2 overexpression in the rhabdomyosarcoma cell line abrogates C6-ceramide-mediated *p21^{Cip1/Waf1}* induction, G2/M arrest and apoptosis.¹⁶

Some reports have demonstrated that p53 acts upstream of ceramide in tumor stress responses. For example, Dbaibo et al. showed that p53 is implicated in N-SMase activation and ceramide formation in response to low concentrations of actinomycin D or γ -irradiation in Molt-4 cells.¹⁷ In other studies, p53 is shown to be a downstream target of ceramide. Indeed, inhibition of p53 expression with antisense oligonucleotides prevented the induction of caspase activity, the increase of BAX and the decrease of Bcl-2 levels, suggesting that p53 acts upstream of Bcl-2, BAX and caspases in the proapoptotic signaling pathway induced by ceramide.¹⁸ Still, other observations place ceramide and p53 in two separate and independent pathways in the apoptotic process.¹¹ For example, treatment with a genotoxin generates ceramide in p53^{+/+} cells (LM cells) as well as in p53^{-/-} cells (LME6).¹⁹ Taken together, it remains unclear how ceramide and p53 are linked in programmed cell death. Moreover, it seems to be cell type-dependent.¹¹

Finally, the position of ceramide with respect to Bcl-2 is variably reported. A number of groups have shown that ceramide is upstream of Bcl-2 in the apoptotic pathway, since Bcl-2 overexpression rescues cells from death induced by ceramide²⁰ or by ceramidase inhibitors.²¹ On the other hand, other studies have demonstrated that Bcl-2 and Bcl-X_L overexpression prevent ceramide formation in response to etoposide, cisplatin and TNF- α in C6 rat glioma and in human U87 glioblastoma cells.²² These observations were attributed to the indirect inhibition of N-SMase. Thus, Bcl-2 can also act upstream of ceramide.

The main objective of the current study was to identify new proteins involved in the apoptotic pathway triggered by ceramide. To achieve this goal, a 2D-DIGE proteomic approach was chosen in order to compare the proteome of adenocarcinoma cells treated or not with long-chain ceramide. Particular attention was paid to proteins involved in the ceramide-p53 pathway to try to better understand the intracellular responses to stress.

Materials and Methods

Cell Culture, Biological Reagents, and Treatments. HCT116 human colon carcinoma cells (ATCC CCL 247) were cultured in McCoy's 5A modified medium (Cambrex, Inc., IA) supplemented with 10% fetal bovine serum, 1% L-glutamine

(200 mM), 100 units/mL penicillin and 100 μ g/mL streptomycin. The cells were maintained at 37 °C in a 5% CO₂ atmosphere. C16-ceramide was obtained from Acros Organics (Geel, Belgium) and dissolved in ethanol. To allow the entrance of long-chain ceramide in the cell, dodecan was added to the medium (0.02%). For all experiments, an equal amount of solvent (ethanol/dodecan) was added to control cultures (i.e., untreated cells) compared to the corresponding ceramide treated conditions. For transfection experiments, control cells were transfected with empty plasmid or GFP siRNA. Cell treatments were performed with 12 μ M C16-ceramide, except in Figure 1B where various concentrations were used.

Protein Extraction and Western Blot Analysis. HCT116 cells were scraped and centrifuged at 1000g for 5 min. The pellets were washed two times with ice-cold PBS. Proteins extracts were prepared by lysing the cells in sodium dodecyl sulfate (SDS) 1%. The cells were vortexed and protein extracts were obtained after 10 min of boiling (Figures 1D, 3, 5B-D, 6B,D,F). Protein concentrations were measured with the Micro BCA protein assay reagent kit (Pierce, Rockford, IL). Proteins were separated by sodium dodecyl sulfate (SDS)-polyacrylamide gel electrophoresis and transferred to polyvinylidene difluoride membranes. After blocking, the membranes were incubated with the monoclonal anti-PARP and anti-Btf antibodies (BD Biosciences Pharmingen, CA). The anti-caspase 3 and anti- α -tubulin antibodies were from Alexis (Lausen, Switzerland) and Sigma (St. Louis, MO). Stratifin was detected with a mouse monoclonal antibody from Abcam (Cambridge, U.K.). The anti-serine 70 phospho-Bcl-2 (δ Bcl-2), anti-prohibitin, anti-Mdm2, and anti-p53 antibodies were purchased from Santa Cruz, whereas stathmin was revealed with rabbit polyclonal antibody (Cell Signaling, Danvers, MA). The anti-BAX antibody was purchased from Calbiochem (San Diego, CA). The membranes were incubated with 1:10 000 diluted peroxidase-conjugated anti-mouse and anti-rabbit secondary antibodies (GE Healthcare, Uppsala, Sweden). The reactions were revealed with the enhanced chemiluminescence detection reagent (ECL kit, Thermo Scientific, MA). Western blottings were performed in triplicate and analyzed by densitometry (Supporting Information Figure S2). The intensity of each band was measured with the Quantity One Software (BioRad, Hercules, CA). To normalize protein levels, the value of the band corresponding to each protein level was divided by the intensity of the corresponding α -tubulin used as an internal standard.

Determination of Apoptosis by Cytochemical Staining. HCT116 cells were seeded at 2×10^4 cells/chamber in eight chamber slides for cytochemical staining and treated or not with C16-ceramide (12 μ M) for 6 h. After treatment, cells were washed with PBS and incubated for 15 min with propidium iodide and Annexin-V (Annexin-V FLUOS Staining kit, Roche, Germany). Cells were visualized with confocal microscopy.

Two-Dimensional Differential In-Gel Electrophoresis (2D-DIGE). **1. CyDye Labeling.** Proteins were extracted by adding lysis buffer containing 50 mM Tris, pH 7.5, 100 mM NaCl, 5 mM EDTA, 0.1% Triton X100, 7 M Urea, 4% CHAPS (v/v), 50 mM DTT, and protease inhibitors (Complete, Roche), followed by vortexing. Cellular debris was removed by centrifugation for 15 min at 20 000g. Total proteins were precipitated using a 2D Clean-up kit (GE Healthcare, Sweden) in order to remove the excess of Tris-HCl, NaCl, EDTA, and DTT that interferes with Cy-labeling. The pH was adjusted to 8.5 with 100 mM NaOH after reconstitution in a minimal volume of labeling buffer (7 M urea, 2 M thiourea, 2% (w/v) ASB 14, 30

mM Tris-HCl, pH 8.5). Protein concentration was evaluated with PlusONE 2-D Quant Kit from GE Healthcare.

To perform an accurate comparative proteomic analysis, the 2D-DIGE procedure, initially developed by Unlu et al. was performed.²³ Twenty-five micrograms of protein extracts of treated cells (12 μ M C16-ceramide during 6 h) and of control cells was labeled separately with 0.2 nmol of CyDye (Cy3, Cy5) (GE Healthcare), vortexed, and incubated 30 min in the dark. The reaction was stopped with 10 mM lysine. A Cy2-stained pooled sample composed of all individual preparations of total proteins constituted an internal standard used to match and normalize gels as described previously.^{24,25} Experiments were performed in triplicate (3 independent control and 3 independent treated cell extracts). Gel multiplexing was obtained by mixing 25 μ g each of one Cy3- and one Cy5-stained sample supplemented with 25 μ g of Cy2-stained internal standard. The volume of the combined labeled samples was adjusted to 450 μ L with standard rehydration buffer (7 M urea, 2 M thiourea, 2% (w/v) ASB 14 and 0.6% (v/v) pH 3–10 NL IPG buffer). The mixed CyDye-labeled samples were used to rehydrate 24 cm IPG strips (pH 3–10 NL) for 12 h at 20 °C and under constant voltage (50 V). Isoelectric focusing (IEF) was successively carried out at 200 V for 1 h, 500 V for 1 h, 1 kV for 1 h and 8 kV for 6 h at 20 °C and a maximum current setting of 50 μ A per strip in an IPGphor isoelectric focusing unit (GE Healthcare). Prior to second-dimension separation, the IPG strips were equilibrated according to Görg et al.²⁶ and then sealed with 0.5% agarose in SDS running buffer on top of 12% (w/v) acrylamide gels. The gels were poured between low-fluorescence glass plates to minimize background fluorescence during scanning. The second-dimension electrophoresis was performed overnight at 20 °C in an Ettan Dalt II system (GE Healthcare) at 1 W/gel. Each gel was then scanned with the Typhoon 9400 scanner (GE Healthcare) at the wavelengths corresponding to each CyDye.

2. Image Analysis. Images were analyzed with the DeCyder software (GE Healthcare) according to the manufacturer. In brief, the three CyDye-labeled forms of each spot were co-detected within each gel and ratios between samples and internal standard abundance were calculated for each spot with the DIA (Differential In-gel Analysis) software module. An average of 3000 spots was detected on each gel. Then, intergel variability was corrected using the internal standard spot maps by the BVA (Biological Variance Analysis) module of the DeCyder software. Protein spots that showed a statistically significant ($p < 0.05$) Student's *t* test for an increase or decrease in normalized spot volume were accepted as being differentially expressed between the compared extracts. The validity of these changes was then confirmed by visual inspection of the gels. This led to the identification of 51 significant protein spot changes between control and treated samples that were subsequently submitted to sequencing by LC-MS/MS.

3. In-Gel Trypsin Digestion and MS-MS Analysis. Spots with a significant variation in their abundance were automatically excised from the gel with the Ettan Spot Picker (GE Healthcare) and underwent tryptic digestion. Spots were washed and desalting in 50 mM ammonium bicarbonate/methanol (50% v/v), followed by acetonitrile (75% v/v, ACN); spots were then digested with Trypsin Gold (MS grade, Promega, WI, 10 mg·mL⁻¹ in 20 mM ammonium bicarbonate) using the Ettan Digester robot (GE Healthcare) from the Ettan Spot Handling workstation. Automated spotting of the samples was carried out with the spotter of the same Workstation (GE Healthcare). Peptides dissolved in 50% ACN containing 0.5% TFA (0.7 μ L) were spotted on MALDI-TOF

disposable target plates (4800, Applied Biosystems, CA) prior to the deposit of 0.7 μ L of α -cyano-4-hydroxycinnamic acid (CHCA) (7 mg/mL, 50% v/v ACN, 0.1% v/v TFA, Sigma Aldrich, MO). Peptide mass determinations were carried out using the Applied Biosystems 4800 Proteomics Analyzer (Applied Biosystems, Foster City, CA). Both PMF and MS/MS in reflectron mode analyses were carried out with the samples. Calibration was carried out with the peptide mass calibration kit for 4700 Proteomics Analyzer (Applied Biosystems). Proteins were identified by searching against the NCBI databases using MASCOT (Matrix Science, www.matrixscience.com, London, U.K.). All searches were carried out using a mass window of 100 ppm and with "*Homo sapiens*" as taxonomy in NCBI database (<http://www.ncbi.nlm.nih.gov/>) and 0.5 Da of tolerance on MS/MS fragments. The search parameters allowed fixed modifications for cysteine (carboxymidomethylation) and methionine (oxidation) and variable modifications on tryptophan (double oxidation or kynurenin) as well as peptide N-terminal E or Q as pyroGlu. Two missed cleavages were allowed and the peptide charge was set at +1. All the identifications were manually verified and validated.

RNA Interference. For RNA interference, decreased Btf expression was obtained by transfecting an ON-TARGETplus SMARTpool siRNA (Dharmacon, CO) using lipofectamine reagent according to the protocol provided by the manufacturer (Invitrogen, CA).

Transient Transfection and Luciferase Assays. For plasmid transfection experiments (Figure 6C), HCT116 cells were seeded in 6-well plates and transfected with MDM2 promoter-driven luciferase or TP53 promoter-driven luciferase reporter constructs and GFP-Btf expression vector (a gift from Dr. T. Haraguchi, Kansai Advanced Research Center, Kobe, Japan) using lipofectamine reagent with a 1:2.5 DNA/lipofectamine ratio, according to the manufacturer's instructions. Plasmid DNA amounts were normalized with the corresponding empty plasmids. Cells were harvested 24 h after transfection.

For Btf depletion experiments (Figure 6E), colon cancer cells were seeded in 6-well plates and cotransfected with MDM2 promoter-driven luciferase reporter construct together with GFP siRNA or Btf siRNA and left untreated or treated with C16-ceramide during 1, 3, or 6 h. Cells were harvested 48 h after transfection.

For all those transfection experiments, luciferase assays were performed with a commercial kit (Roche) and luciferase activity was measured in a luminescence microplate (Wallac Victor 2 multilabel counter plate, Perkin-Elmer, MA) and corrected for the protein concentration in the sample by Bradford's protein determination.

Determination of Cell Viability. HCT116 cells were seeded at 10⁴ cells/well in flat-bottom 96 well plates (Greiner Bio-one, Belgium). Cell viability was assessed by reduction of the yellow tetrazolium salt (MTS) to the blue formazan product by mitochondrial enzymes in viable cells ("Cell Titer 96 Aqueous", Promega, The Netherlands). At the end of the treatment period, 20 μ L of MTS/PMS solution was added to each well. The reactions were incubated for 2 h at 37 °C in a humidified atmosphere of 5% CO₂. Absorbance was then measured at 492 nm with a spectrophotometer and the data were expressed as a percentage of absorbance observed in untreated control cells (Figure 1A,B).

For plasmid transfection experiments (Figure 4A), HCT116 cells were seeded in 96-well plates (1 \times 10⁴ cells/well) and transfected with the GFP-Btf expression vector or with the corresponding empty plasmid using lipofectamine reagent

according to the manufacturer's instructions. For Btf depletion experiments (Figure 4B), colon cancer cells were seeded in 96-well plates (5000 cells/well) and transfected with GFP siRNA or Btf siRNA using lipofectamine reagent. For all those transfection experiments, viability was measured using the CellTiter-Glo Luminescent Cell Viability Assay (Promega, Madison, WI), according to the manufacturer's instructions.

Caspases 3/7 Cleavage. HCT116 cells were seeded in 96-well plates (5000 cells/well) and transfected with GFP siRNA or Btf siRNA using lipofectamine reagent. Cells were left untreated or treated with C16-ceramide for 3 and 6 h. Apoptosis was measured by quantification of both caspases 3 and 7 activities, using the luminometric Caspase-Glo 3/7 assay (Promega, Madison, WI), according to the manufacturer's protocol.

Statistics. Statistical analysis was performed by *t*-test using Prism 4.00 Software (Graph pad, San Diego, CA), with statistical significance accepted at $P < 0.05$.

Results

Incorporating C16-ceramide in HCT116 Cells Decreases Cell Viability. Short length ceramides are not constitutively expressed in HCT116 cell lines.²⁷ However, C16-, C20-, C22- and C24-ceramides were detected by reverse-phase chromatography coupled with tandem mass spectrometry.²⁷ Among them, C16- and C24-ceramides appeared to be the predominant subtype found in HCT116.

To mimic the biological effect of endogenous ceramide, HCT116 cells were stimulated with C16-ceramide in the presence of dodecan to allow the entrance of the lipid into the cells. As shown in Figure 1A,B, cell viability strongly decreased in a time- and concentration-dependent manner after C16-ceramide treatment. About 60% of cells survived after 6 h of treatment with 12 μ M of C16-ceramide. In these conditions, a 2-fold increase of C16-ceramide cell content was measured by mass spectrometry after 15 min of cell contact (data not shown). Similarly C20-, C22- and C24-ceramides also decreased HCT116 cell viability (data not shown).

A double staining with Annexin V/propidium iodide confirmed the induction of apoptosis and necrosis as well as morphological change of the cells after stimulation with C16-ceramide (Figure 1C). As previously demonstrated with C6-ceramide,²⁸ the decrease in cell viability is partly due to apoptosis. Indeed, our data showed that PARP cleavage increased while pro-caspase 3 decreased after 3 and 6 h of C16-ceramide treatment, respectively (Figure 1D).

2D-DIGE Analysis Allows the Identification of 51 Proteins Differentially Expressed in C16-ceramide Treated versus Control HCT116 Cells. A differential proteomic analysis was undertaken to identify the proteins involved in the C16-ceramide-dependent pathways in the HCT116 adenocarcinoma cell line. Proteins from control and C16-treated cells (12 μ M, 6 h) were extracted from six independent cultures (3 controls and 3 treated). Both control and treated cell extracts were labeled with Cy3 and Cy5 to account for any protein-labeling bias. A Cy2-stained pool of all samples was used as internal standard.

Following electrophoresis, spots were resolvable in images generated from Cy2, Cy3 and Cy5 fluorescence of the labeled proteins. The 2D-gels were highly reproducible and gave well-resolved spots with little streaking (Supporting Information Figure S1). It was found that out of approximately 3000 detectable spots, 73 underwent significant up- or down-regulation after C16-ceramide stimulation, with control versus

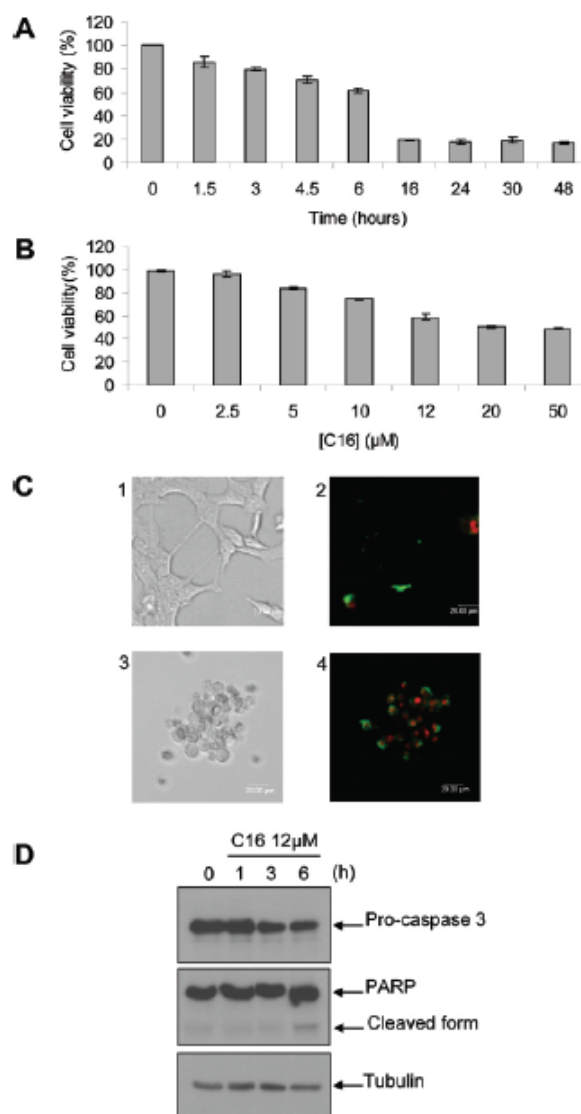


Figure 1. Incorporated C16-ceramide in HCT116 cells induced toxicity. (A) HCT116 cells were seeded in 96-well plates in triplicate and treated with 12 μ M C16-ceramide during 1.5, 3, 4.5, 6, 16, 24, 30, and 48 h. Cell viability was estimated with MTS reduction assay ($n = 6$). (B) HCT116 cells were seeded in 96-well plates in triplicate and treated for 6 h with C16-ceramide at different concentrations (2.5, 5, 10, 12, 20, 50 μ M). Cell viability was estimated with MTS reduction assay ($n = 6$). (C) Double staining with Annexin V and propidium iodide from untreated cells (2) or HCT116 cells treated with C16-ceramide (12 μ M) during 6 h (4). (1) and (3) are the corresponding phase contrast images. Annexin-V (green) is a marker of apoptosis and propidium iodide (red) reflects the permeability of the cell membrane, thereby serving as a marker of necrosis. Bar = 20 μ m. (D) Caspase-3 activation and PARP cleavage by C16-ceramide. HCT116 were treated or not with ceramide (12 μ M) for various time (1, 3, 6 h). Twenty micrograms of total cell lysates was separated on SDS-polyacrylamide gels, and immunoblotting was revealed with anti-caspase 3 and PARP antibodies. Each membrane was probed with anti- α -tubulin antibodies to ensure equal protein loading.

treated spot volume ratios of at least 1.5-fold within the 95th confidence level (Student's *t* test, $P < 0.05$) (Figure 2).

All the 73 protein spots were excised from the preparative gel, digested with trypsin and analyzed using mass spectrometry. Fifty-one out of 73 analyzed protein spots yielded unambiguous identifications using MASCOT database searching

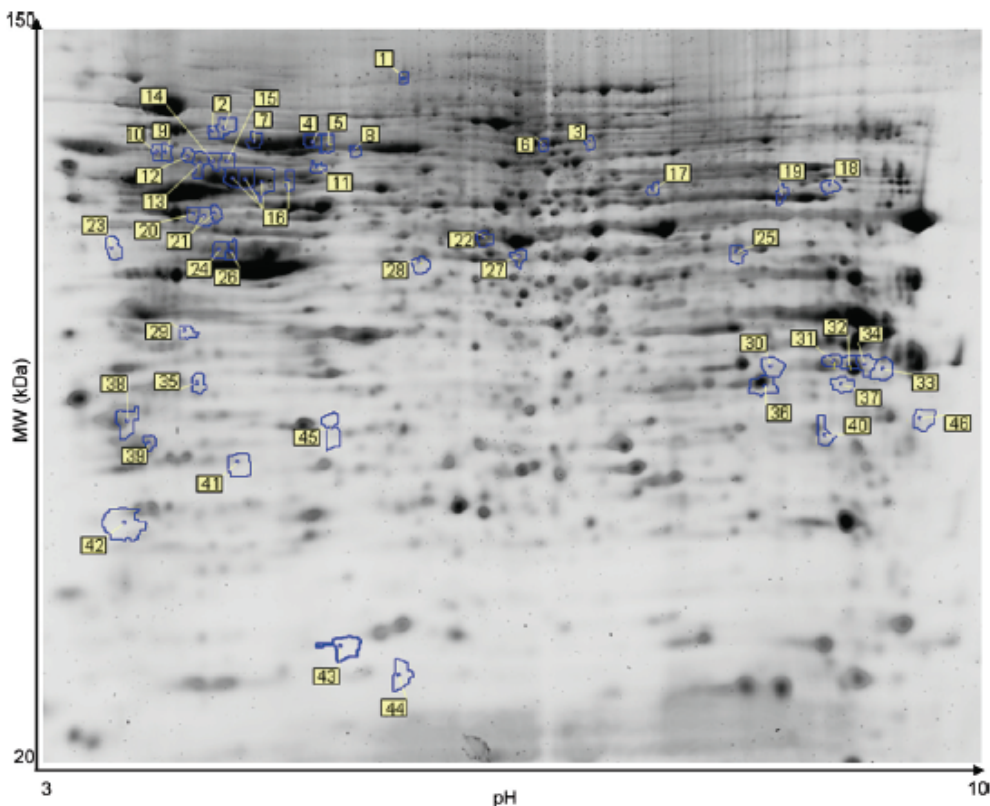


Figure 2. Two-dimensional preparative gel. 2D-DIGE revealed 73 protein spots differentially expressed in C16-ceramide treated or untreated HCT116 cells. Labeled samples (25 μ g of each Cy2, Cy3, and Cy5) were loaded on 24 cm, 3–10 NL IPG-strips and subjected to isoelectric focusing. Second-dimension was performed in 12% acrylamide gels. Gels were scanned and subsequent image analyses were performed. Proteins were identified from 51 spots that were found to vary significantly ($p < 0.05$, Student's *t* test) in treated cells compared to untreated cells.

program. Table 1 lists the proteins that were identified by MS/MS (Supporting Information Table S1). Several functional groups of proteins were affected, including regulators of transcription and translation, proteins involved in cytoskeleton organization, metabolism and response to stress.

Confirmation of 2D-DIGE Results for Some Proteins Involved in the p53 Pathway. As C16-ceramide is able to induce apoptosis, proteins known to be involved in the p53 signaling pathway were studied. Western Blotting (WB) experiments were performed to validate some of the data obtained by 2D-DIGE analysis. As shown in Figure 3 and in Supporting Information Figure S2, the levels of stratifin (2.77-fold, $p < 0.0001$) and stathmin (1.11-fold, $p = 0.002$) decreased after 6 h of ceramide treatment as compared to untreated cells, whereas the expression of prohibitin (1.48-fold, $p = 0.002$) and Btf (1.24-fold, $p = 0.0139$) increased as shown by 2D-DIGE analysis (Table 1).

Ceramide Induces Apoptosis through Btf. Among the differentially expressed proteins after ceramide treatment, Btf (Bcl-2-associated transcription factor) was of particular interest as its level of expression was increased 1.85-fold by measurement of spot abundance in 2D gels and this increase was confirmed by WB after ceramide treatment (Figure 3D). Btf is a newly discovered transcriptional repressor that induces cell death upon overexpression.²⁹

The transfection of GFP-Btf expression plasmid induced a 20% decrease in cell viability when compared to GFP empty vector ($p = 0.0045$) (Figure 4A). In addition, Btf-depleted cells were found to be more resistant to death triggered by ceramide (Figure 4B). Indeed, cell viability was increased (19.4% at 3 h

and 13.8% at 6 h) for Btf-depleted cells compared to GFP siRNA transfected cells after 3 and 6 h of C16-ceramide treatment ($p = 0.0188$, 6 h).

To determine if Btf is involved in ceramide-dependent apoptosis, HCT116 cells were transfected with GFP siRNA and Btf siRNA, followed by treatment with ceramide. Our results showed that knocking down Btf decreased caspases 3/7 activities (up to 60%) in colon cancer cells in response to 3 and 6 h of C16-ceramide treatment (Figure 4C) ($p < 0.0001$, 6 h).

C16-ceramide and Btf Expression Up-Regulate p53 and BAX Expression. Liu et al. provided evidence that disruption of Btf-mediated TP53 gene transcription leads to suppression of TP53-mediated apoptosis in response to DNA damage.³⁰ This suggests that Btf induces apoptosis in a TP53-dependent manner.

In our HCT116 model, C16-ceramide treatment generated a significant increase (3-fold) in TP53 promoter activity as measured by the luciferase reporter gene assay (Figure 5A). This resulted in an early increase of p53 expression within 15 min of C16-ceramide treatment ($p = 0.0178$ at 15 min; $p = 0.0049$ at 30 min) as compared to HCT116 cells treated with actinomycin D used as positive control (Figure 5B). Actinomycin D is a well-known inducer of p53 pathway. It binds DNA at the transcription initiation complex and prevents elongation by RNA polymerase.

To investigate whether Btf is implicated in the ceramide-p53 dependent pathway, a GFP-Btf expression plasmid was transfected in HCT116 cells and proteins involved in the p53 apoptotic pathway were quantified by WB. As shown in Figure 5C, p53 and BAX protein levels increased (1.33-fold, $p = 0.0057$

Table 1. List of Proteins Identified by MS/MS That Are Differentially Expressed in HCT116 Treated or Not with C16-ceramide

functions/protein name	protein symbol	ID SPROT	theo. MW (Da) ^a	theo. pI ^a	exp. MW (Da) ^b	exp. pI ^b	fold ^c	P-value ^e	no. of peptides	sequence coverage %	spot number ^d
Protein Transport											
ADP-ribosylation factor 3	ARF3	P61204	20601	6.84	15410	5.75	2.13	0.013	4	40.9	43
Mannose-6-phosphate receptor-binding protein 1	M6PBP	O60664	47047	5.3	50371	5.02	2.28	0.0078	2	10.8	24
Rab GDP dissociation inhibitor alpha	CDIA	P31150	50583	5.00	66383	5.01	2.02	0.0066	4	15	14
Cell Proliferation/Apoptosis											
Prohibitin	PHB	P35232	29804	5.57	30831	5.66	1.73	0.019	5	29.4	45
14-3-3 protein sigma (stratifin)	14335	P31947	27774	4.68	28493	4.51	-1.53	0.013	3	19.7	39
Annexin A1	ANXA1	P04083	38714	6.57	32821	8.54	1.8	0.0015	3	14.4	37
Protein Folding/Response to Stress											
78 kDa glucose regulated-protein	GRP78	P11021	72333	5.07	72333	5.07	2.25	0.00029	8	23.1	2 (a)
Calumenin	CALU	O43852	37107	4.47	50645	4.41	-2.17	0.0038	8	23.1	2 (b)
Annexin A2	ANXA2	P07355	38604	7.57	34987	8.64	2.58	0.025	4	16.2	23
T-complex protein 1 subunit delta	TCPD	P50991	57924	7.96	60768	8.44	1.51	0.0024	7	33.9	34
Stress-70 protein, mitochondrial	GRP75	Q1HFB43	73680	5.87	72321	5.54	1.99	0.022	5	17.1	18
60 kDa heat shock protein, mitochondrial	CH60	P10809	61055	5.7	72124	5.67	1.61	0.0042	4	10.4	4
Channel											
Heat shock 70 kDa protein 1	HSP71	P08107	70052	5.48	70285	5.79	1.74	0.0008	8	20.5	5
Heat shock 70 kDa protein 8 isoform 1 variant	Q53GZ6	70899	5.28	72321	5.54	1.99	0.022	4	14.3	16 (a)	
Heat shock protein 75 kDa, mitochondrial	TRAP1	Q12931	80110	8.30	71247	5.23	1.66	0.0095	8	27.9	16 (b)
Stathmin	STMN1	P16949	17302	5.76	80834	6.98	1.73	0.0069	7	26.2	16 (c)
Adenylyl cyclase-associated protein	Q5JPF8	43539	5.61	71538	6.85	1.52	0.0026	4	9.4	16 (d)	
Voltage-dependent anion-selective channel protein 1	VDAC1	P21796	30773	8.62	35515	8.58	1.61	0.027	8	11.2	8
Voltage-dependent anion-selective channel protein 2	VDAC2	P45890	31566	7.50	30773	8.62	1.52	0.043	4	44.2	4
					36246	8.11	1.55	0.013	2	30.8	32
									2	47.3	33
									2	11.4	30

Table 1 Continued

functions/protein name	protein symbol	ID SPOT	theo. MW (Da) ^a	theo. pF ^b	exp. MW (Da) ^b	exp. pF ^b	fold ^c	P-value ^c	no. of peptides	sequence coverage %	spot number ^d
Voltage-dependent anion-selective channel protein 3	VDAC3	Q9Y277	30659	8.84	30045	8.98	1.72	0.022	3	18	46
Glycerol-3-phosphate dehydrogenase, mitochondrial	GPDM	P43304	80853	7.58	80834	6.98	1.73	0.0069	4	7.8	3
ATP synthase subunit alpha, mitochondrial	ATPA	P25705	59751	9.16	60768	8.44	1.51	0.0024	2	6.1	18
Citrate synthase, mitochondrial	CISY	O75390	51712	8.45	51712	8.45	1.64	0.0073	6	18.8	19
Adenosylhomocysteinase	SAHH	P23526	47716	5.92	58951	6.49	1.73	0.0092	8	27.3	21 (a)
L-lactate dehydrogenase A chain	LDHA	P00338	36689	8.44	35708	8.49	2.43	0.0019	5	27.3	21 (b)
Hydroxacyl-coenzyme A dehydrogenase, mitochondrial	HCDH	Q16836	34278	8.88	35515	8.58	1.61	0.0086	6	17.4	25
Adenylate kinase 2, mitochondrial	KAD2	P54819	26478	7.67	28223	8.46	-1.64	0.019	6	20.6	27
Mitochondrial-processing peptidase subunit beta	MPPB	O75439	54366	6.38	52397	6.54	-1.58	0.0013	5	30.1	31
Glucose-6-phosphate 1-dehydrogenase	G6PD	P11413	59257	6.39	61182	7.44	-1.77	0.00051	4	14.3	32
Elongation factor 1-beta	EF1B	P24534	24764	4.5	24764	4.5	-1.53	0.011	3	47.3	40
Elongation factor 1-gamma	EF1G	P26641	50119	6.25	52397	6.54	-1.58	0.0013	4	12.1	22
Elongation factor 1-delta	Q4VBZ6	28558	4.81	39435	4.76	-1.8	0.012	8	47.1	29	
Bd-2-associated transcription factor (Btf)	BCLF1	Q9NYF8	106122	9.99	90125	6.75	1.85	0.0015	2	2.5	1
ATP-dependent DNA helicase 2, subunit 1	KU70	P12956	69843	6.23	71538	6.85	1.52	0.0026	4	11	6
Histone-binding protein RBBP7	Q16576	47820	4.89	56851	4.87	1.65	0.011	7	27	20	
Heterogeneous nuclear ribonucleoprotein G	HNRPG	P38159	42332	10.1	48357	6.19	1.86	0.00017	3	13.8	28
Heterogeneous nuclear ribonucleoprotein K	HNRPK	P61978	50976	5.39	66113	5.09	1.61	0.011	2	6.9	15
40S ribosomal protein S3	RS3	P23396	26688	9.68	32866	8.1	1.51	0.043	4	27.6	36

Table 1 Continued

functions/protein name	protein symbol	ID SPOT	MW (Da) ^a	theo. pI ^a	Ubiquitination	MW (Da) ^b	exp. pI ^b	fold ^c	P-value ^c	no. of peptides	sequence coverage ^c %	spot number ^d
26S proteasome non-ATPase regulatory subunit 12	PSD12	O00232	52904	7.53	59460	8.15	1.64	0.0073	3	8.55	19	
Calcyclin-binding protein	CYBP	Q9HB71	26210	8.28	28223	8.46	-1.64	0.019	3	33.3	40	
Ubiquillin-1	UBQL1	Q9UMX0	62519	5.02	67384	4.68	1.91	0.028	6	20.5	10	
Serine/ threonine-protein phosphatase 2A 56 kDa regulatory subunit beta isoform	2A5B	Q15173	57393	6.27	67384	4.73	1.86	0.038	5	19.1	9	
Serine/ threonine-protein phosphatase 2A 65 kDa regulatory subunit A alpha isoform	2AAA	P30153	65309	5.00	67109	4.86	2.02	0.023	6	19.5	12	
Ras GTPase-activating protein-binding protein 1	G3BP1	Q13283	52164	5.36	67475	5.58	-1.89	0.005	6	26.2	11	
Ran-specific GTPase-activating protein	RANG	P43487	23310	5.19	23310	5.19	-1.61	0.016	4	27.9	41	
Others												
NSFL1 cofactor p47 Membrane-associated progesterone receptor component 1	NSFL1C PGRC1	Q9UNZ2 O00264	40573 21671	4.99 4.56	50371 22643	5.02 4.43	2.28 1.86	0.0078 0.039	3 2	14 17	24 42	
Annexin A5	ANXA5	P08758	35937	4.94	33361	4.8	1.84	0.0011	4	22.8	35	
Actin, cytoplasmic 2	ACTG	P63261	41793	5.31	49623	5.09	3.11	0.025	5	20.8	26	
					48357	6.19	1.86	0.00017	3	13.6	28	

^a Theo. MW and pI correspond to theoretical values. ^b Exp. MW and pI correspond to experimental calculated values. Molecular weight and isoelectric points were calculated by DeCyder software. ^c Fold is the ratio between the protein expression level of C16 treated cells and the protein expression level of control cells. ^d Spot numbers correspond to the numbers given in Figure 2. ^e $p < 0.05$; (a), (b), (c), (d), indicated spots giving rise to the same identification and located on the gel from the left to the right.

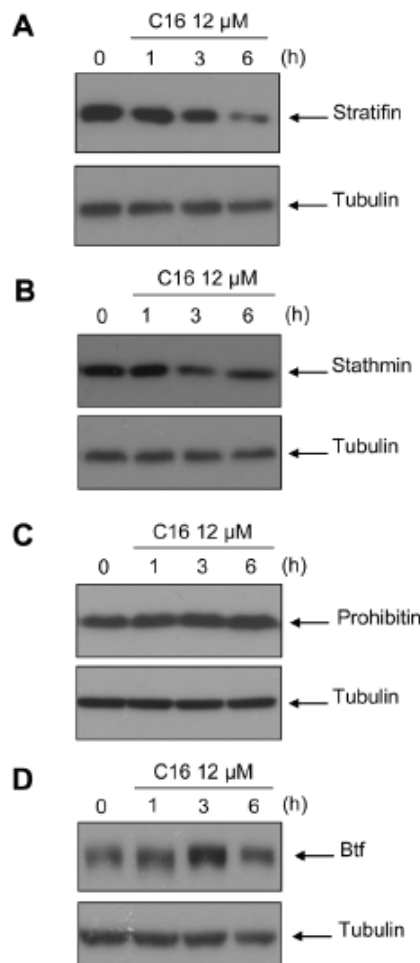


Figure 3. Validation of the 2D-DIGE data by Western blotting of HCT116 cells treated by C16-ceramide. HCT116 cells were left untreated or stimulated with C16-ceramide (12 μ M) during 1, 3, and 6 h. Twenty micrograms of total cell lysates was separated on SDS-PAGE gel, and immunoblotting was performed with anti-stratifin (A), -stathmin (B), -prohibitin (C), and -Btf (D) antibodies together with anti-tubulin antibodies as loading control. A representative Western blot is shown for each case.

and 1.38-fold, $p = 0.0260$, respectively), whereas phospho-Bcl-2 level decreased (1.22-fold, $p = 0.0141$) after transfection of the Btf expression plasmid. Moreover, in HCT116 cells, both endogenous Btf and pBcl-2 are located in the nucleus in basal conditions (Figure S3A). After ceramide treatment (12 μ M, 3 h, Figure S3B), Btf and pBcl-2 localization remained in the nucleus. This strengthens the hypothesis that they could physically interact, even if this can only be demonstrated by immunoprecipitation. This has been already tested without success, maybe due to the poor Btf solubility in IP buffers.

As shown in Figure 5D, RNAi-mediated Btf depletion also partially inhibited BAX expression after ceramide treatment indicating that Btf could be an intermediate in the ceramide-p53 pathway. All these data suggest that Btf acts as a proapoptotic factor.

C16-ceramide Down-Regulates Mdm2 Expression via Btf. Downstream targets and mechanisms of Btf-induced apoptosis remain poorly understood. Since Btf was shown to bind DNA,²⁹ we investigated whether it could modulate transcription, as one report suggested that MDM2 could be a Btf target gene.²⁹ HCT116 cells were transfected with the MDM2-LUC reporter plasmid containing 5' regulatory regions

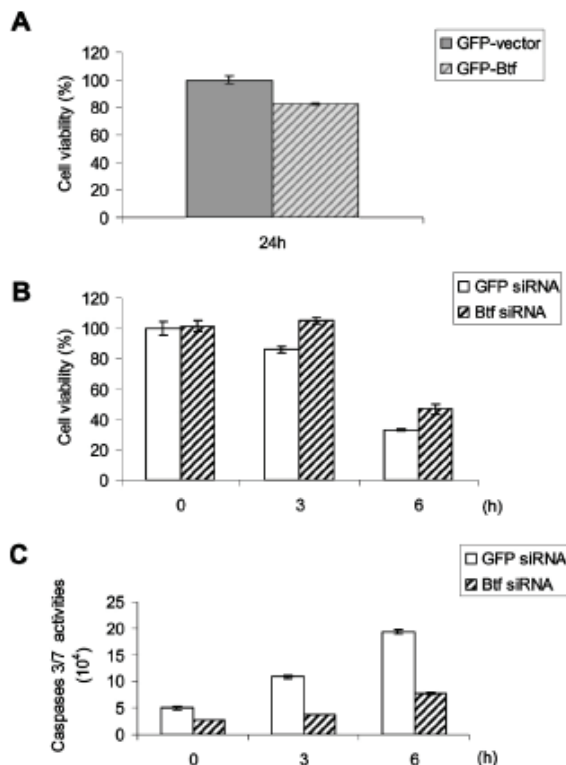


Figure 4. Ceramide induces apoptosis through Btf. (A) Btf overexpression decreases cell viability. HCT116 cells were transfected with GFP-vector or GFP-Btf (0.1 μ g). Cell viability was measured 24 h post-transfection. (B) Down-regulation of endogenous Btf enhances cell viability. HCT116 cells were transfected with GFP siRNA or Btf siRNA and were left untreated or treated with C16-ceramide for 3 and 6 h. Cell viability was measured 48 h post-transfection. (C) Btf silencing diminishes ceramide-induced cell apoptosis in colon cancer cells. HCT116 cells were transfected with GFP siRNA or Btf siRNA and were left untreated or treated with C16-ceramide for 3 and 6 h. Cellular apoptosis was quantified 48 h post-transfection by assessing caspases 3/7 activities.

of the MDM2 gene. As shown in Figure 6A, after 6 h of C16-ceramide (12 μ M) treatment, LUC activity decreased significantly compared to untreated cells. Mdm2 protein expression levels also decreased significantly after 6 h of C16-ceramide treatment (1.85-fold, $p = 0.0002$) (Figure 6B). Altogether, these data suggest that C16-ceramide could repress the MDM2 gene transcription.

Moreover, the MDM2-LUC plasmid was cotransfected with Btf expression plasmid (Figure 6C). A significant decrease in luciferase activity (40%) was observed. These data suggest that MDM2 gene expression is negatively regulated by Btf family members. Western blotting showed in parallel that Mdm2 protein expression decreased significantly after Btf plasmid transfection (1.30-fold, $p = 0.0022$) (Figure 6D).

HCT116 cells were cotransfected with the MDM2 promoter reporter luciferase construct and the GFP siRNA or Btf siRNA. Btf silencing increased the activity of the MDM2 promoter after ceramide treatment (Figure 6E). This result demonstrates that Btf negatively regulates Mdm2 expression. To further confirm this finding, HCT116 cells were transfected with GFP siRNA or Btf siRNA followed by treatment with ceramide. This result demonstrated that, in the presence of Btf siRNA, Mdm2 protein expression was induced after 30 min and 1 h of ceramide treatment (Figure 6F).

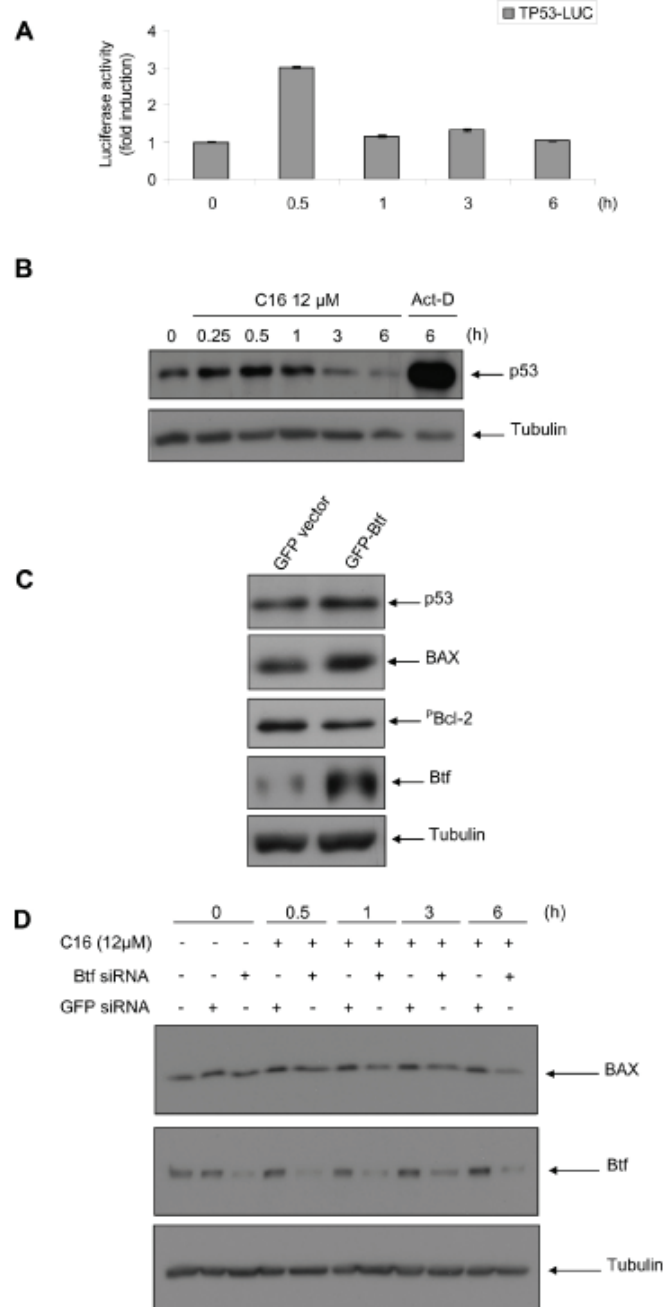


Figure 5. C16-ceramide and Btf expression upregulate p53 and BAX expression. (A) C16-ceramide increases TP53 promoter activity after 30 min of treatment. HCT116 cells were transiently transfected with 0.2 μ g of TP53-LUC and then left untreated or treated with C16-ceramide for the indicated times. The luciferase activity was measured 24 h post-transfection. (B) C16-ceramide up-regulates p53 expression. HCT116 cells were left untreated or stimulated with C16-ceramide (12 μ M) for the indicated period of times or with actinomycin D (Act-D) for 6 h. Protein extracts were subjected to Western Blotting probed with anti-p53 and α -tubulin antibodies. (C) Btf overexpression increases the p53 and BAX protein expressions and decreases pBcl-2 in HCT116 cells. HCT116 cells were transfected with GFP-vector or GFP-Btf (0.5 μ g) during 24 h. Cell lysates were analyzed by immunoblotting with anti-p53, pBcl-2, -Btf, and -BAX antibodies, as well as with anti-tubulin as loading control. (D) Down-regulation of endogenous Btf modifies BAX expression in a time-dependent manner. HCT116 cells were transfected with GFP siRNA or Btf siRNA and then stimulated with C16-ceramide for 30 min, 1, 3, and 6 h. Cell extracts were subjected to anti-BAX, -Btf and α -tubulin antibodies for Western blot analysis.

Discussion

In this study, we report that C16-ceramide, a lipid second messenger, induces a decrease in viability of adenocarcinoma cells (HCT116), partly due to apoptosis, as demonstrated by PARP cleavage and caspase-3 activation. The molecular mechanisms involved in ceramide signaling pathway were investigated using a 2D-DIGE proteomic analysis of cells treated with the long-chain C16-ceramide. Among the 51 identified differentially expressed proteins, some are thought to be involved in p53 signaling pathway, namely, prohibitin, stratifin, stathmin and Btf. The modulation of their expression by ceramide was confirmed by Western blotting.

As far as we know, those proteins have not yet been reported to be involved in the ceramide signaling pathway and are thus discussed here in relation with the apoptosis observed after cell ceramide treatment (Figure 7).

Our data showed that stathmin expression level decreased after ceramide treatment. Stathmin (oncoprotein 18) is a cytosolic protein that destabilizes microtubules through tubulin sequestration and/or promotion of microtubule disruption.³¹ Johnsen and colleagues have identified stathmin as being repressed by p53 in p53-mediated G2/M cell-cycle arrest.³² Furthermore, knockdown of stathmin partially restored cell-cycle regulation and activation of apoptosis.³³ Singer et al. also demonstrated that inhibition of stathmin expression leads to reduced viability and migration of HCC cells.³⁴ In our 2D-DIGE proteomic analysis and WB experiments, a decrease of stathmin protein levels was observed after C16-ceramide treatment (Figure 7). This decrease correlated with the apoptosis observed after C16-ceramide treatment despite the fact that further investigations should be undertaken to determine the role of p53 in the stathmin signal triggered by ceramide.

In our study, prohibitin protein level was found to be increased after ceramide treatment (Figure 7) suggesting its involvement in the ceramide-p53 signaling pathway by a mechanism that remains to be characterized. In the literature, prohibitin was found to physically interact with Rb as well as E2F family members in mammalian cells.³⁵ Furthermore, studies showed that prohibitin could physically interact with and enhance the transcriptional activity of p53.³⁶ These results suggested that prohibitin could regulate cell proliferation and apoptosis by affecting the transcriptional activity of E2F1 and p53.³⁶

Our data also showed that stratifin expression level decreased after ceramide treatment. Stratifin has been shown to have a clear impact on Mdm2 activity and p53 stabilization.^{37,38} While studying the molecular mechanism of this increased stabilization of p53, it was found that stratifin antagonized the biological functions of Mdm2 by blocking Mdm2-mediated p53 ubiquitination and nuclear export. In addition, stratifin could facilitate the oligomerization of p53 and enhanced p53 transcriptional activity. As a target gene of p53, stratifin appears to have a positive feedback effect on p53 activity (Figure 7).³⁷ The decrease in stratifin expression obtained in this study after C16-ceramide treatment is somewhat controversial, but confirms our previous work with C6-ceramide.³⁹ In our model of colon cancer cells, stratifin may play a minor role in the regulation of p53.

In the present study, Btf was found, for the first time, to be implicated in the apoptotic signal triggered by ceramide (Figures 3D and 4C). This protein was found to be upstream of well-known apoptosis-related proteins such as Mdm2, BAX and Bcl-2 (Figures 5C and 6D).

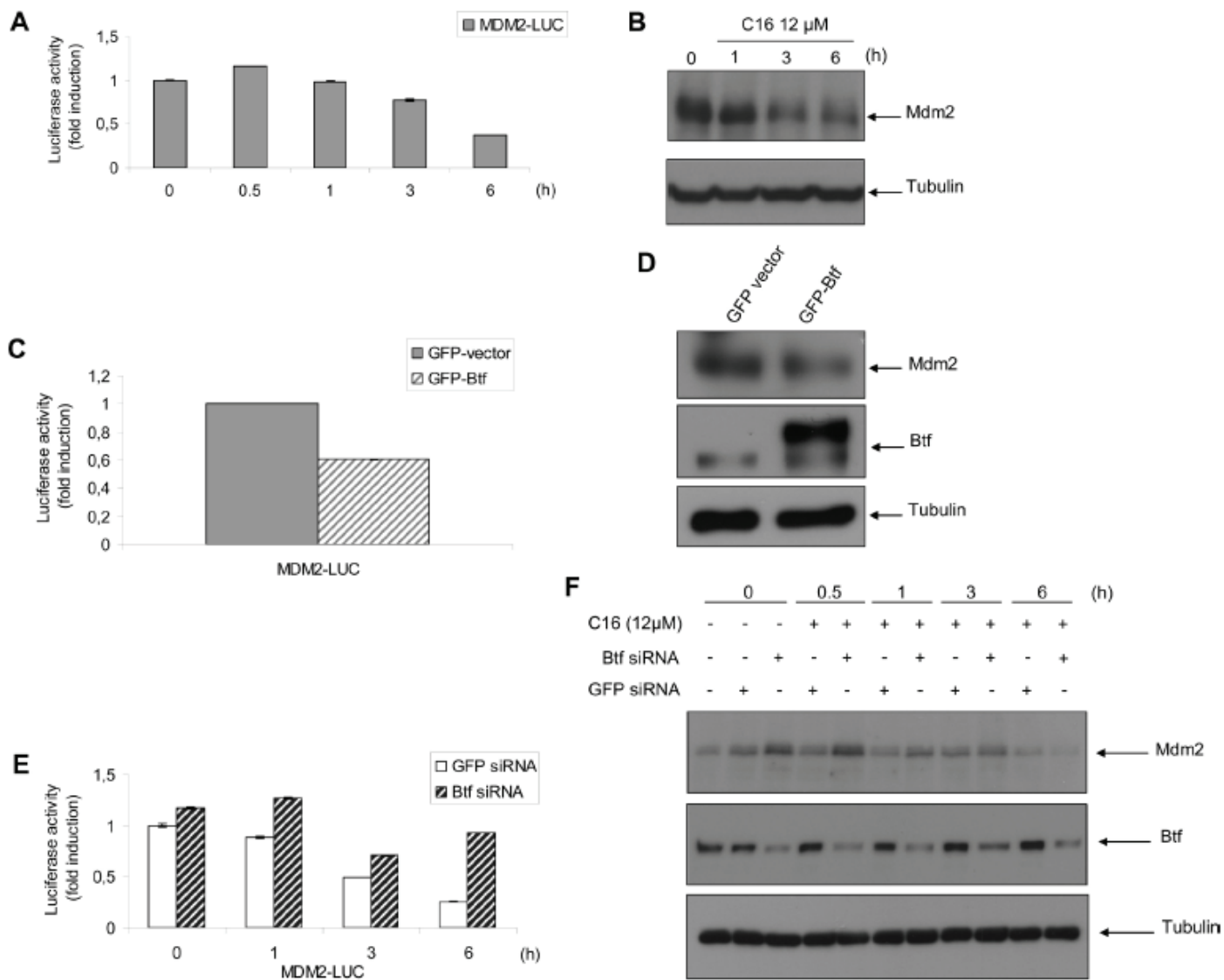


Figure 6. C16-ceramide and Btf expression down-regulate Mdm2 expression. (A) C16-ceramide decreases the MDM2 promoter activity. HCT116 cells were transiently transfected with 0.5 μ g of MDM2-LUC and then left untreated or treated with C16-ceramide for 30 min, 1, 3, and 6 h. The luciferase activity was measured 24 h post-transfection. The increase in luciferase activity is expressed in fold induction relative to the activity obtained with cells transfected with empty vector. (B) C16-ceramide decreases Mdm2 protein levels in colon cancer cells. These cells were left untreated or stimulated with C16-ceramide (12 μ M) for 1, 3, and 6 h. Cell extracts were subjected to immunoblot analysis with anti-Mdm2 or - α -tubulin. (C) Btf overexpression decreases the MDM2 promoter activity. Colon cancer cells were cotransfected with 0.5 μ g of MDM2 promoter reporter construct together with 0.5 μ g of GFP-vector or GFP-Btf. The luciferase activity was measured 24 h post-transfection. (D) Btf overexpression decreases the Mdm2 protein expression in HCT116 cells. These cells were transfected with GFP-vector or GFP-Btf (2 μ g) during 24 h. Cell lysates were analyzed by immunoblotting with anti-Mdm2, -Btf, and - α -tubulin antibodies. (E) Down-regulation of endogenous Btf enhances the MDM2 promoter activity. HCT116 cells cotransfected with 0.5 μ g of MDM2 promoter reporter construct and GFP siRNA or Btf siRNA were left untreated or treated with C16-ceramide for 1, 3, or 6 h. The luciferase activity was measured 48 h post-transfection. (F) Down-regulation of endogenous Btf modifies Mdm2 expression in a time-dependent manner. HCT116 cells were transfected with GFP siRNA or Btf siRNA and then stimulated with C16-ceramide for 30 min, 1, 3, and 6 h. Cell extracts were subjected to anti-Mdm2, -Btf, and - α -tubulin antibodies for Western blotting analysis.

Btf (Bcl-2-associated transcription factor, also named BCLAF1) is a nuclear protein that was originally identified in a yeast two-hybrid screen against the adenoviral bcl-2 homologue E1B19K and was shown to interact with Bcl-2 and Bcl-x_L.²⁹ Btf was also described to promote apoptosis when overexpressed in HeLa cells,²⁹ the responsible mechanism being largely unknown. However, in a recent study, Btf (or BCLAF1)-deficient thymocytes and splenocytes exposed to gamma-irradiation or etoposide failed to show any defect in cell death compared with *wild-type* cells. The authors showed that Btf is not required for thymocyte development but is essential for homeostasis of

T- and B-cells and activation-induced proliferation of T cells.⁴⁰ In another study, Liu et al. demonstrated that suppression of transcriptional activation by Btf silencing diminished TP53-dependent apoptosis, implying that regulation of Btf by PKC δ also has a critical role in determining cell fate with DNA damage.³⁰ Beside this, Kasof hypothesized, but never demonstrated, that Btf may repress the transcription of survival genes; one possible target being the p53 inhibitor, Mdm2.²⁹ Mdm2 is known to bind directly to the transactivation domain of p53, and abrogates the transactivational activity of p53.⁴¹ Mdm2 also promotes the degradation of p53 via its ubiquitin E3 ligase

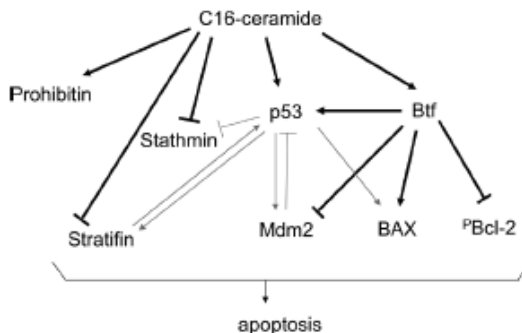


Figure 7. Proteins involved in the apoptotic response to C16-ceramide treatment. 2D-DIGE analysis revealed the involvement of Btf, prohibitin, stratifin and stathmin in the ceramide signaling pathway. C16-ceramide was found to induce p53 expression. Ceramide also decreases Mdm2 expression via Btf up-regulation. Moreover, overexpression of Btf increases BAX and p53 and decreases phospho-Bcl-2 expression. These regulations result in increased apoptosis. Arrows in bold represent new interactions suggested by our study; gray arrows represent known data coming from the literature.

activity, which leads to degradation by the proteasome. Mdm2 is furthermore a direct transcriptional target of p53 and is up-regulated upon p53 activation, leading to a negative feedback loop.⁴²

Possible intermediates between ceramide and Btf are not yet known. Btf contains more than 30 phosphorylation sites identified by mass-spectrometry,⁴³ but little is known about kinases that target this protein. Liu et al. demonstrated that PKC-delta interacted with Btf to co-occupy CPE-TP53.³⁰ Another study by Linding et al. identified Btf as a novel target of GSK-3beta.⁴⁴ In our study, two kinases were investigated, namely, PKC-delta and GSK-3beta but they were not found to be involved in the ceramide-Btf pathway in our colon cancer cell model (data not shown). Further investigations have to be undertaken to determine which kinases are implicated in the Btf signal triggered by ceramide.

The expression of Mdm2 decreased significantly after ceramide treatment and after Btf overexpression in colon cancer cells (Figures 6B,D and 7). Moreover, Btf silencing increases MDM2 promoter activity in response to C16-ceramide (Figure 6E). Thus, these results suggest that Btf is required for transcriptional regulation of MDM2 gene. Our results also indicate that Btf decreases the phosphorylated form of Bcl-2. Previous studies showed that Bcl-2 or Bcl-x_L, two antiapoptotic members of the Bcl-2 family, abrogated Btf-mediated transcriptional repression, probably by binding to and sequestering Btf in the cytoplasm.²⁹ Thus, these studies, combined with our report, may provide a feedback loop between Btf and Bcl-2.

Taken together, our proteomic data demonstrate for the first time the implication of Btf, and other proteins like prohibitin, stratifin and stathmin, in the ceramide signaling pathway. Ceramides are known to induce cell death, but the molecular mechanism involved is still largely unclear. Our study showed that those second messengers significantly decrease intracellular levels of Mdm2 and phospho-Bcl-2 through the increase of Btf expression, whereas levels of p53 and BAX were found to be increased. Interestingly, Btf silencing leads to an increase in resistance of cells to ceramide treatment indicating that Btf plays an important role in the ceramide-mediated cell death. All these results give new insights into the ceramide apoptosis signaling pathway.

The better understanding of the complex network of sphingolipid signaling is very important in cancer therapy. The identification of all the components involved in the ceramide pathway may help to characterize new targets as well as facilitate the development of novel strategies to face drug resistance.

Abbreviations: 2D-DIGE, two-dimensional differential gel electrophoresis; ACN, acetonitrile; Btf, Bcl-2-associated transcription factor; DTT, dithiothreitol; EDTA, ethylenediaminetetraacetic acid; IEF, isoelectric focusing; IPG, immobilized pH gradient; MALDI-TOF-MS, matrix-assisted laser desorption/ionization-mass spectrometry; PBS, phosphate buffer saline; PMF, peptide mass fingerprint; SDS, sodium dodecyl sulfate; TOF, time-of-flight.

Acknowledgment. M.F. and P.L. are Research Associates and M.-P.M. is Senior Research Associate at F.R.S.-FNRS (National Fund for Scientific Research). J.P. is Research Director at FNRS. We thank the “Centre Anti-Cancéreux” (Liège, Belgium), the FNRS, the “Fonds Léon Frédéricq” (Liège, Belgium), the “Télévie” for their financial supports. We thank to Dr. Alain Chariot for helpful discussions and critical reading of the manuscript. The authors are grateful to Dr. J. C. Marine for providing MDM2-LUC plasmid and to Dr. T. Haraguchi for the GFP-Btf plasmid.

Supporting Information Available: Table listing the proteins identified by MS/MS; 2D-DIGE experiment; Western blottings; endogenous Btf expression in HCT116 cells and colocalization with pBcl-2 in the nucleus. This material is available free of charge via the Internet at <http://pubs.acs.org>.

References

- Billlich, A.; Baumrucker, T. Sphingolipid metabolizing enzymes as novel therapeutic targets. *Subcell Biochem.* 2008, **49**, 487–522.
- Hannun, Y. A.; Obeid, L. M. Principles of bioactive lipid signalling: lessons from sphingolipids. *Nat. Rev. Mol. Cell Biol.* 2008, **9** (2), 139–50.
- Saddoughi, S. A.; Song, P.; Ogretmen, B. Roles of bioactive sphingolipids in cancer biology and therapeutics. *Subcell Biochem.* 2008, **49**, 413–40.
- Lin, C. F.; Chen, C. L.; Lin, Y. S. Ceramide in apoptotic signaling and anticancer therapy. *Curr. Med. Chem.* 2006, **13** (14), 1609–16.
- Siskind, L. J. Mitochondrial ceramide and the induction of apoptosis. *J. Bioenerg. Biomembr.* 2005, **37** (3), 143–53.
- Samsel, L.; Zaidel, G.; Drungoole, H. M.; Jelovac, D.; Drachenberg, C.; Rhee, J. G.; Brodie, A. M.; Bielawska, A.; Smyth, M. J. The ceramide analog, B13, induces apoptosis in prostate cancer cell lines and inhibits tumor growth in prostate cancer xenografts. *Prostate* 2004, **58** (4), 382–93.
- Pettus, B. J.; Chalfant, C. E.; Hannun, Y. A. Ceramide in apoptosis: an overview and current perspectives. *Biochim. Biophys. Acta* 2002, **1585** (2–3), 114–25.
- Swanton, C.; Marani, M.; Pardo, O.; Warne, P. H.; Kelly, G.; Sahai, E.; Elustondo, F.; Chang, J.; Temple, J.; Ahmed, A. A.; Brenton, J. D.; Downward, J.; Nicke, B. Regulators of mitotic arrest and ceramide metabolism are determinants of sensitivity to paclitaxel and other chemotherapeutic drugs. *Cancer Cell* 2007, **11** (6), 498–512.
- Bielawska, A.; Bielawski, J.; Szulc, Z. M.; Mayroo, N.; Liu, X.; Bai, A.; Elojemy, S.; Rembiesa, B.; Pierce, J.; Norris, J. S.; Hannun, Y. A. Novel analogs of D-e-MAPP and B13. Part 2: signature effects on bioactive sphingolipids. *Bioorg. Med. Chem.* 2008, **16** (2), 1032–45.
- Sultan, I.; Senkal, C. E.; Ponnusamy, S.; Bielawski, J.; Szulc, Z.; Bielawska, A.; Hannun, Y. A.; Ogretmen, B. Regulation of the sphingosine-recycling pathway for ceramide generation by oxidative stress, and its role in controlling c-Myc/Max function. *Biochem. J.* 2006, **393** (Pt 2), 513–21.
- Taha, T. A.; Mullen, T. D.; Obeid, L. M. A house divided: ceramide, sphingosine, and sphingosine-1-phosphate in programmed cell death. *Biochim. Biophys. Acta* 2006, **1758** (12), 2027–36.
- Marine, J. C.; Dyer, M. A.; Jochemsen, A. G. MDMX: from bench to bedside. *J. Cell Sci.* 2007, **120** (Pt 3), 371–8.

(13) Hara, S.; Nakashima, S.; Kiyono, T.; Sawada, M.; Yoshimura, S.; Iwama, T.; Banno, Y.; Shinoda, J.; Sakai, N. p53-Independent ceramide formation in human glioma cells during gamma-radiation-induced apoptosis. *Cell Death Differ.* 2004, 11 (8), 853–61.

(14) Jin, Y.; Lee, H.; Zeng, S. X.; Dai, M. S.; Lu, H. MDM2 promotes p21waf1/cip1 proteasomal turnover independently of ubiquitylation. *EMBO J.* 2003, 22 (23), 6365–77.

(15) Zhang, Z.; Wang, H.; Li, M.; Agrawal, S.; Chen, X.; Zhang, R. MDM2 is a negative regulator of p21WAF1/CIP1, independent of p53. *J. Biol. Chem.* 2004, 279 (16), 16000–6.

(16) Phillips, D. C.; Hunt, J. T.; Moneypenny, C. G.; Maclean, K. H.; McKenzie, P. P.; Harris, L. C.; Houghton, J. A. Ceramide-induced G2 arrest in rhabdomyosarcoma (RMS) cells requires p21 Cip1/Waf1 induction and is prevented by MDM2 overexpression. *Cell Death Differ.* 2007, 14 (10), 1780–91.

(17) Dbaibo, G. S.; Pushkareva, M. Y.; Rachid, R. A.; Alter, N.; Smyth, M. J.; Obeid, L. M.; Hannun, Y. A. p53-dependent ceramide response to genotoxic stress. *J. Clin. Invest.* 1998, 102 (2), 329–39.

(18) Kim, S. S.; Chae, H. S.; Bach, J. H.; Lee, M. W.; Kim, K. Y.; Lee, W. B.; Jung, Y. M.; Bonventre, J. V.; Suh, Y. H. P53 mediates ceramide-induced apoptosis in SKN-SH cells. *Oncogene* 2002, 21 (13), 2020–8.

(19) Yang, J.; Duerksen-Hughes, P. J. Activation of a p53-independent, sphingolipid-mediated cytolytic pathway in p53-negative mouse fibroblast cells treated with N-methyl-N-nitro-N-nitrosoguanidine. *J. Biol. Chem.* 2001, 276 (29), 27129–35.

(20) Zhang, J.; Alter, N.; Reed, J. C.; Borner, C.; Obeid, L. M.; Hannun, Y. A. Bcl-2 interrupts the ceramide-mediated pathway of cell death. *Proc. Natl. Acad. Sci. U.S.A.* 1996, 93 (11), 5325–8.

(21) Raisova, M.; Goltz, G.; Bektas, M.; Bielawska, A.; Riebeling, C.; Hossini, A. M.; Eberle, J.; Hannun, Y. A.; Orfanos, C. E.; Geilen, C. C. Bcl-2 overexpression prevents apoptosis induced by ceramidase inhibitors in malignant melanoma and HaCaT keratinocytes. *FEBS Lett.* 2002, 516 (1–3), 47–52.

(22) Sawada, M.; Nakashima, S.; Banno, Y.; Yamakawa, H.; Takenaka, K.; Shinoda, J.; Nishimura, Y.; Sakai, N.; Nozawa, Y. Influence of Bax or Bcl-2 overexpression on the ceramide-dependent apoptotic pathway in glioma cells. *Oncogene* 2000, 19 (31), 3508–20.

(23) Unlu, M.; Morgan, M. E.; Minden, J. S. Difference gel electrophoresis: a single gel method for detecting changes in protein extracts. *Electrophoresis* 1997, 18 (11), 2071–7.

(24) Alban, A.; David, S. O.; Bjorkesten, L.; Andersson, C.; Sloge, E.; Lewis, S.; Currie, I. A novel experimental design for comparative two-dimensional gel analysis: two-dimensional difference gel electrophoresis incorporating a pooled internal standard. *Proteomics* 2003, 3 (1), 36–44.

(25) Knowles, M. R.; Cervino, S.; Skynner, H. A.; Hunt, S. P.; de Felipe, C.; Salim, K.; Meneses-Lorente, G.; McAllister, G.; Guest, P. C. Multiplex proteomic analysis by two-dimensional differential in-gel electrophoresis. *Proteomics* 2003, 3 (7), 1162–71.

(26) Gorg, A.; Boguth, G.; Obermaier, C.; Posch, A.; Weiss, W. Two-dimensional polyacrylamide gel electrophoresis with immobilized pH gradients in the first dimension (IPG-Dalt): the state of the art and the controversy of vertical versus horizontal systems. *Electrophoresis* 1995, 16 (7), 1079–86.

(27) Fillet, M.; Van Heugen, J. C.; Servais, A. C.; De Graeve, J.; Crommen, J. Separation, identification and quantitation of ceramides in human cancer cells by liquid chromatography-electrospray ionization tandem mass spectrometry. *J. Chromatogr. A* 2002, 949 (1–2), 225–33.

(28) Fillet, M.; Bentires-Alj, M.; Deregowski, V.; Greimers, R.; Gielen, J.; Piette, J.; Bours, V.; Merville, M. P. Mechanisms involved in exogenous C2- and C6-ceramide-induced cancer cell toxicity. *Biochem. Pharmacol.* 2003, 65 (10), 1633–42.

(29) Kasof, G. M.; Goyal, L.; White, E. Btf, a novel death-promoting transcriptional repressor that interacts with Bcl-2-related proteins. *Mol. Cell. Biol.* 1999, 19 (6), 4390–404.

(30) Liu, H.; Lu, Z. G.; Miki, Y.; Yoshida, K. Protein kinase C delta induces transcription of the TP53 tumor suppressor gene by controlling death-promoting factor Btf in the apoptotic response to DNA damage. *Mol. Cell. Biol.* 2007, 27 (24), 8480–91.

(31) Steinmetz, M. O. Structure and thermodynamics of the tubulin-stathmin interaction. *J. Struct. Biol.* 2007, 158 (2), 137–47.

(32) Johnsen, J. I.; Aurelio, O. N.; Kwaja, Z.; Jorgensen, G. E.; Pellegata, N. S.; Plattner, R.; Stanbridge, E. J.; Cajot, J. F. p53-mediated negative regulation of stathmin/Op18 expression is associated with G(2)/M cell-cycle arrest. *Int. J. Cancer* 2000, 88 (5), 685–91.

(33) Alli, E.; Yang, J. M.; Hait, W. N. Silencing of stathmin induces tumor-suppressor function in breast cancer cell lines harboring mutant p53. *Oncogene* 2007, 26 (7), 1003–12.

(34) Singer, S.; Ehemann, V.; Brauckhoff, A.; Keith, M.; Vreden, S.; Schirmacher, P.; Breuhahn, K. Protumorigenic overexpression of stathmin/Op18 by gain-of-function mutation in p53 in human hepatocarcinogenesis. *Hepatology* 2007, 46 (3), 759–68.

(35) Wang, S.; Nath, N.; Fusaro, G.; Chellappan, S. Rb and prohibitin target distinct regions of E2F1 for repression and respond to different upstream signals. *Mol. Cell. Biol.* 1999, 19 (11), 7447–60.

(36) Fusaro, G.; Dasgupta, P.; Rastogi, S.; Joshi, B.; Chellappan, S. Prohibitin induces the transcriptional activity of p53 and is exported from the nucleus upon apoptotic signaling. *J. Biol. Chem.* 2003, 278 (48), 47853–61.

(37) Yang, H. Y.; Wen, Y. Y.; Chen, C. H.; Lozano, G.; Lee, M. H. 14-3-3 sigma positively regulates p53 and suppresses tumor growth. *Mol. Cell. Biol.* 2003, 23 (20), 7096–107.

(38) Lee, M. H.; Lozano, G. Regulation of the p53-MDM2 pathway by 14-3-3 sigma and other proteins. *Semin. Cancer Biol.* 2006, 16 (3), 225–34.

(39) Fillet, M.; Cren-Olive, C.; Renert, A. F.; Piette, J.; Vandermoere, F.; Rolando, C.; Merville, M. P. Differential expression of proteins in response to ceramide-mediated stress signal in colon cancer cells by 2-D gel electrophoresis and MALDI-TOF-MS. *J. Proteome Res.* 2005, 4 (3), 870–80.

(40) McPherson, J. P.; Sarras, H.; Lemmers, B.; Tamblyn, L.; Migon, E.; Matysiak-Zablocki, E.; Hakem, A.; Azami, S. A.; Cardoso, R.; Fish, J.; Sanchez, O.; Post, M.; Hakem, R. Essential role for Bclaf1 in lung development and immune system function. *Cell Death Differ.* 2009, 16 (2), 331–9.

(41) Wade, M.; Wahl, G. M. Targeting Mdm2 and Mdmx in cancer therapy: better living through medicinal chemistry. *Mol. Cancer Res.* 2009, 7 (1), 1–11.

(42) Slack, A.; Chen, Z.; Tonelli, R.; Pule, M.; Hunt, L.; Pession, A.; Shohet, J. M. The p53 regulatory gene MDM2 is a direct transcriptional target of MYCN in neuroblastoma. *Proc. Natl. Acad. Sci. U.S.A.* 2005, 102 (3), 731–6.

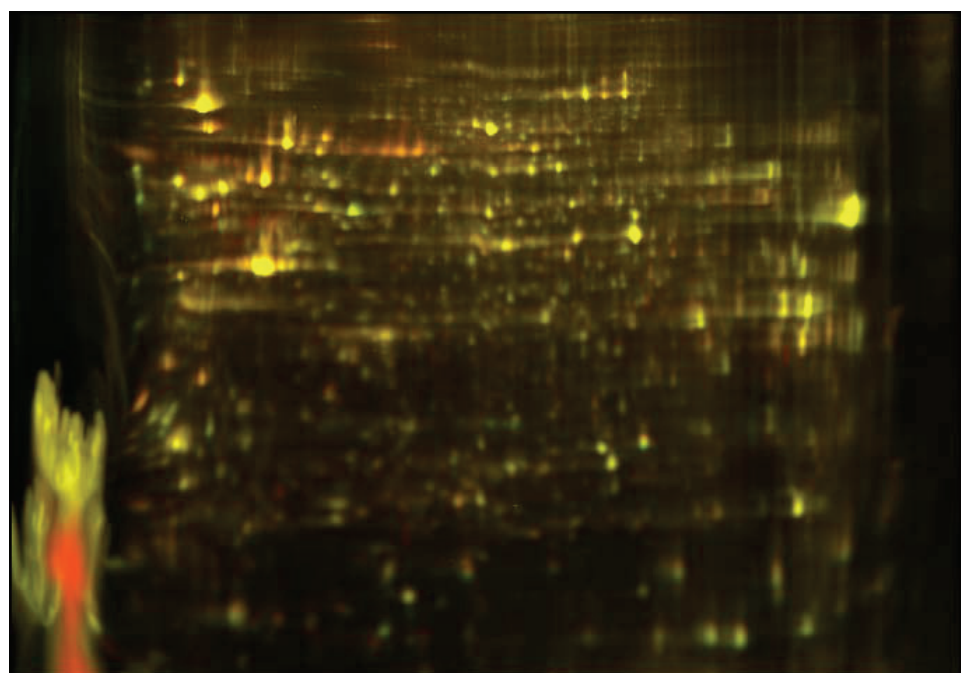
(43) Diella, F.; Cameron, S.; Gemund, C.; Linding, R.; Via, A.; Kuster, B.; Sicheritz-Ponten, T.; Blom, N.; Gibson, T. J. PhosphoELM: a database of experimentally verified phosphorylation sites in eukaryotic proteins. *BMC Bioinf.* 2004, 5, 79.

(44) Linding, R.; Jensen, L. J.; Ostheimer, G. J.; van Vugt, M. A.; Jorgensen, C.; Miron, I. M.; Diella, F.; Colwill, K.; Taylor, L.; Elder, K.; Metalnikov, P.; Nguyen, V.; Pasculescu, A.; Jin, J.; Park, J. G.; Samson, L. D.; Woodgett, J. R.; Russell, R. B.; Bork, P.; Yaffe, M. B.; Pawson, T. Systematic discovery of in vivo phosphorylation networks. *Cell* 2007, 129 (7), 1415–26.

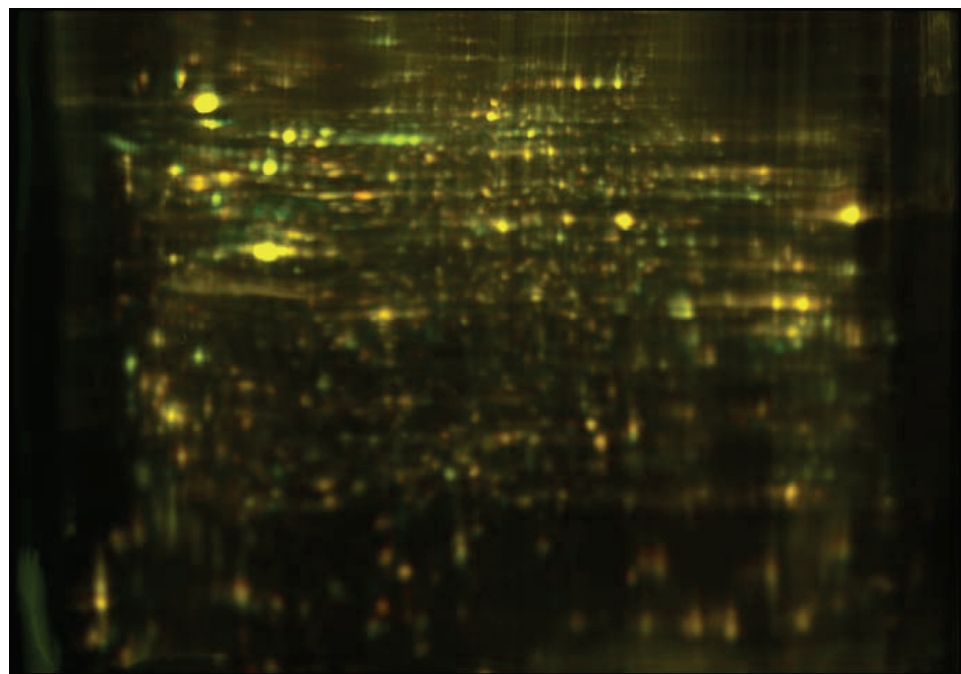
PR9005316

Supporting information related to the manuscript

(a)



(b)



(c)

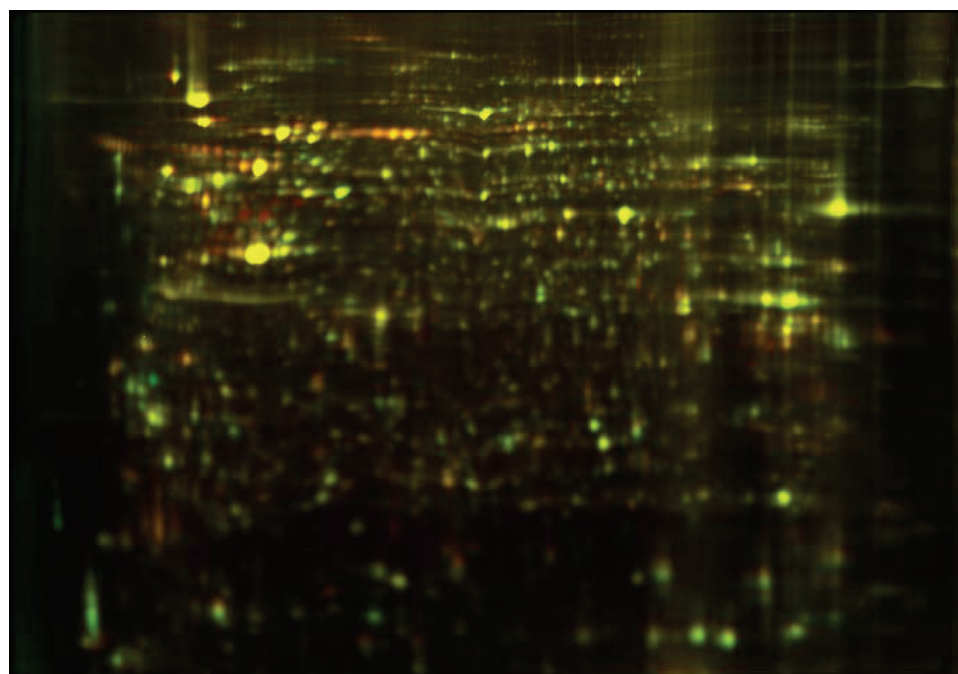


Figure S1. 2D-DIGE experiment. Overlay of the two dye scan-images (Cy3 and Cy5) in triplicates. We interchanged Cy3 and Cy5 labeling to avoid dye labeling-bias. **(a)** Scan-images of Cy3 control cells and Cy5 treated cells. **(b)** Scan-images of Cy5 control cells and Cy3 treated cells. **(c)** Scan-images of Cy3 control cells and Cy5 treated cells.

Table S1. List of proteins identified by MS/MS with their sequenced peptide sequences, ion score and spot number.

Functions/protein name	Peptides sequences	Ion score	Spot number
Protein transport			
ADP-ribosylation factor 3	R.VNEAREELMR.M K.NISFTVWDVGGQDK.I + DOUBLE Ox (W) K.QDLPNAMNAAEITDKLGLHSLR.H R.HYFQNTQGLIFVVDNSNDRER.V	20 23 8 12	43
Mannose-6-phosphate receptor binding protein 1	R.IATSLDGFDVASVQQQR.Q M.SADGAEADGSTQVTVEEPVQQPSVVDR.V + Acetyl (N-term)	74 30	24
Rab GDP dissociation inhibitor alpha	R.FQLLEGPPESMGR.G R.MAGTAFDFENMKR.K K.FLVFVANFDENDPK.T K.SPYLYPLYGLGELPQGFAR.L	3 15 64 37	14
Cell proliferation/apoptosis			
Prohibitin	R.FDAGELITQR.E R.II.FRPVASQLPR.I R.IFTSIGEDYDER.V R.KLEAAEDIAYQLSR.S K.AAELIANSLATAGDGLIELR.K	16 30 17 27 24	45
14-3-3 protein sigma (stratifin)	R.YLAEVATGDDKKR.I K.SNEEGSEEKGPEVRE K.LAEQAERYEDMAAFMK.G	45 49 33	39
Annexin A1	K.GVDEATIIDLTKRN K.GLGTDEDLIEILASR.T K.GTDVNVFNTILTTR.S	57 79 8	37
Protein folding/response to stress			
78 kDa glucose regulated-protein	R.AKFEELNMDLFR.S R.ITPSYVAFTPEGER.L K.KSDIDEIVLVGGSTR.I	31 69 118	2 (a)
78 kDa glucose regulated-protein	R.IINEPTAAIAYGLDKR.E K.VTHAVVTVPAYFNDAQR.Q K.DNHILLGTFDLTGIPPAAPR.G R.IEIESFYEGEDFSETLTR.A K.VLESDLKKSDIDEIVLVGGSTR.I	107 112 146 158 168	
78 kDa glucose regulated-protein	R.AKFEELNMDLFR.S R.ITPSYVAFTPEGER.L R.IINEPTAAIAYGLDKR.E K.NQLTSPNENTVFDAKR.L K.VTHAVVTVPAYFNDAQR.Q K.DNHILLGTFDLTGIPPAAPR.G R.IEIESFYEGEDFSETLTR.A K.VLESDLKKSDIDEIVLVGGSTR.I	32 25 48 49 38 35 70 67	2 (b)
Calumenin	R.EQFVEFR.D K.TEREQFVEFR.D R.HLVYESDQNKGDKGK.L K.TFDQLTPEESKER.L	13 16 51 47	23
Annexin A2	R.QDIAFAYQR.R K.SLYYYIQQDTK.G K.GVDEVTIVNILTNR.S R.SNAQRQDIAFAYQR.R K.SLYYYIQQDTKGDYQK.A R.RAEDGSVIDYELIDQDAR.D K.AYTNFDAERDALNIETAIK.T	25 35 66 32 42 38 25	34
T-complex protein 1 subunit delta	R.SILKIDDVVNTR.- K.GIHPPTIISESFQK.A K.GAYQDRDKPAQIR.F R.ALIAAGGAPEIELALR.L R.AFADAMEVIPSTLAENAGLNPISTVTEL.R.N	23 93 32 26 45	18
Stress-70 protein, mitochondrial	R.TTPSVVAFTADGER.L K.LLGQFTLIGIPPAAPR.G K.NAVITVPAYFNDSQR.Q K.STNGDTFLGGEDFDQALL.R.H	105 47 29 136	4

Results I

Stress-70 protein, mitochondrial	K.DAGQISGLNVLR.V R.AQFEGIVTDLIR.R K.SDIEVILVGGMTR.M R.AQFEGIVTDLIRR.T K.LLGQFTLIGIPPAPR.G K.NAVITVPAYFNDSQR.Q K.STNGDTFLGGEDFDQALLR.H K.AMQDAEVSKSDIGEVILVGGMTR.M	95 70 35 29 53 80 156 9	5
60 kDa heat shock protein, mitochondrial	R.GYISPYFINTSK.G K.ISSIQSIVPALEIANAHR.K R.IQEIEQLDVTTSEYEKEK.L K.LVQDVANNTNEEAGDGTATVLAR.S	29 15 13 19	16 (a)
	R.GYISPYFINTSK.G R.AAVEEGIVLGGGCALL.R.C K.ISSIQSIVPALEIANAHR.K K.TLNDELEIIEGMKFDR.G R.LKVGLQVVAVKAPGFGDNR.K R.ALMLQGVDLLADAVAVTMGPK.G R.IQEIEQLDVTTSEYEKEK.L R.KPLVIIAEDVDGEALSTLVLR.L	57 48 98 33 43 42 84 83	16 (b)
	R.AAVEEGIVLGGGCALL.R.C K.ISSIQSIVPALEIANAHR.K K.TLNDELEIIEGMKFDR.G R.LKVGLQVVAVKAPGFGDNR.K R.IQEIEQLDVTTSEYEKEK.L R.KPLVIIAEDVDGEALSTLVLR.L K.LVQDVANNTNEEAGDGTATVLAR.S	71 141 50 84 142 117 151	16 (c)
	R.GYISPYFINTSK.G R.AAVEEGIVLGGGCALL.R.C R.IQEIEQLDVTTSEYEKEK.L	32 13 30	16 (d)
Heat shock 70kDa protein 1	R.LVNHFVEEFKR.K R.TTPSYVAFTDTER.L R.IINEPTAAAIAYGLDR.T K.QTQFTTYSQNPGVLIQVYEGER.A	26 23 78 40	8
Heat shock 70kDa protein 8 isoform 1 variant	R.TTPSYVAFTDTER.L R.IINEPTAAAIAYGLDKK.V K.TVTNAVTVPAYFNDSQR.Q K.QTQFTTYSQNPGVLIQVYEGER.A	20 123 132 91	4
	R.TTPSYVAFTDTER.L K.LLQDFNNGKELNK.S K.STAGDTHLGGEDFDNR.M R.IINEPTAAAIAYGLDKK.V K.NQVAMNPTNTVFDAKR.L K.TVTNAVTVPAYFNDSQR.Q K.QTQFTTYSQNPGVLIQVYEGER.A	18 68 55 113 13 110 112	7
Heat shock protein 75 kDa, mitochondrial	R.AQLLQPTLEINPR.H K.YSNFVSPFLYLNGR.R	48 51	3
	K.FFEDYGLFMR.E R.SLYSEKEVFIR.E R.AQLLQPTLEINPR.H R.YESSALPSGQLTLSSEYASR.M	21 49 36 56	6
Cytoskeleton			
Stathmin	R.ASGQAFELILSPRS.S R.SKESVPEFPLSPPK.K	51 62	44
Adenyl cyclase-associated protein	R.SALFAQINQGESITHALK.H K.AGAAPYVQAFDSLLAGPVAEYLK.I	46 47	17
Channel			
Voltage-dependent anion selective channel protein 1	R.VTQSNFAVGYK.T R.GLKLTDFSSFPNTGK.K K.KLETAVNLAWTAGNSNTR.F + DOUBLE Ox (W) K.VNNSSLIGLGYTQTLKPGIK.L M.AVPPTYADLGK.S Acetyl (N-term)	42 80 21 51 23	32
	R.VTQSNFAVGYK.T K.GYGFGLIKLDLK.T R.GLKLTDFSSFPNTGK.K	75 58 93	33

	K.KLETAVNLAWTAGNSNTR.F + DOUBLE Ox (W)	73	
	K.VNNSSLIGLGYTQTLKPGIK.L	99	
	K.TDEFQLHTNVNDGTEFGGSIYQK.V	87	
	M.AVPPTYADLGK.S Acetyl (N-terminus)		
Voltage-dependent anion selective channel protein 2	R.NNFAVGYR.T	53	30
	K.YQLDPTASISAK.V	57	
	R.DIFNKGFGFGLVK.L	93	
	K.LTFDTITFSPNTGKK.S	69	
	K.SINAGGHKVGGLALEA.-	66	
	R.DIFNKGFGFGLVKLDVK.T	76	
	K.VNNSSLIGVGYTQTLRPGVK.L	81	
	R.TGDFQLHTNVNDGTEFGGSIYQK.V	92	
Voltage-dependent anion selective channel protein 3	K.LSQNNFALGYKA	23	46
	K.LTLDTIFVPNTGKK.S	27	
	K.VNNASLIGLGYTQTLRPGVK.L	30	
Enzymatic activity			
Glycerol-3-phosphate dehydrogenase, mitochondrial	K.GFITIVDVQR.V	49	3
	K.AIMKLIDIEQYR.M	34	
	R.LVSEFPYIEAEVK.Y	46	
	R.LAFLNVQAAEEALPR.I	73	
ATP synthase subunit alpha, mitochondrial	K.GIRPAINVGLSVSR.V	18	18
	R.TGAIVDVPVGEELLGR.V	37	
	R.ISVREPMQGTGK.A	17	19
	K.GIRPAINVGLSVSR.V	25	
	R.EAYPGDVFYLHSR.L	46	
	R.ILGADTSVDLEETGR.V	40	
	R.TGAIVDVPVGEELLGR.V	49	
	R.EVAFAQFGSDLDAATQQLLSR.G	24	
	K.AHGGYSVFAVGVGER.T	99	21 (a)
	R.FTQAGSEVSALLGR.I	102	
	K.VALVYQGMNEPPGAR.A	31	
	R.LVLEVAQHLGESTVR.T	91	
	K.VLDSGAPIKIPVGPETLGR.I	102	
	R.AIAELGIYPAVDPLDSTS.R	92	
	R.FLSQPFQVAEVFTGHMGK.L	78	
	R.IPSAVGYQPTLATDMGTMQER.I	14	
ATP synthase subunit alpha, mitochondrial	K.AHGGYSVFAVGVGER.T	115	21 (b)
	R.FTQAGSEVSALLGR.I	83	
	K.VALVYQGMNEPPGAR.A	20	
	R.LVLEVAQHLGESTVR.T	69	
	K.VLDSGAPIKIPVGPETLGR.I	90	
	R.AIAELGIYPAVDPLDSTS.R	108	
	R.FLSQPFQVAEVFTGHMGK.L	69	
	R.IPSAVGYQPTLATDMGTMQER.I	4	
Citrate synthase, mitochondrial	R.ALGFPLERPK.S	15	25
	R.VVPGYGHAVLR.K	31	
	R.ALGVLAQLIWSR.A + DOUBLE Ox (W)	19	
	K.GLVYETSVLDPDEGR.F	22	
	H.ASASSTNLKDILADLIPKEQAR.I	77	
Adenosylhomocysteinase	R.RIILLAEGR.L	20	27
	K.YPQLLPGIR.G	43	
	K.VNIKPQVDR.Y	17	
	K.ALDAEENEMPGLMR.M	17	
	R.KALDIAEENEMPGLMR.M	8	
	K.DGPLNMILDDGGDLTNLIHTK.Y	65	
L-lactate dehydrogenase A chain	K.LVITAGAR.Q	25	31
	R.FRYLMGER.L	13	
	R.QQEGESRLNLVQR.N	18	
	R.NVNIFKFIIPNVVK.Y	58	
	K.IVSGKDYNVTANSKLVITAGAR.Q	8	
	M.ATLKQDQLIYNLLKEEQTPQN.K + Acetyl (N-terminus)	15	
Hydroxyacyl-coenzyme A dehydrogenase, mitochondrial	R.LLVPYLMEAIR.L	6	32
	K.FAENPKAGDEFVEK.T	65	
	R.FAGLHFFNPVPVMK.L	22	
Adenylate kinase isoenzyme 2, mitochondrial	K.NGFLLDGFP.R	35	40
	R.AVLLGPPGAGKGTQAPR.L	34	

Results I

Mitochondrial-processing peptidase subunit beta	M.APSVPAEPEYPKGIR.A R.LQAYHTQTPLIEYYR.K K.EKLDSVIEFSIPDSLLIR.R R.SYHEEFNPKPEPMKDDITGEPLIR.R	18 35 43 10	18 35 43 10
Glucose-6-phosphate 1 dehydrogenase	R.RIPIPELEAR.I R.STQAATQVVLNPETR.V R.AVEILADIQNSTLGEAEIERER.G K.DLVDYITTHYKGPR.I R.IVLAAAGGVSHDELLDLAK.F	16 8 2 41 57	16 8 2 41 57
<i>Transcription/Translation</i>			
Elongation factor 1-beta	K.LVPVGYGIK.K K.LVPVGYGIKK.L K.SPAGLQVLNDYLADK.S	32 32 84	32 32 84
Elongation factor 1- gamma	K.AKDPFAHLPK.S K.STFVLDEFK.R.K K.ALIAAQYSGAQVR.V K.QATENAKEEVRR.I	15 16 52 20	15 16 52 20
Elongation factor 1-delta	R.LRQYAEK.K K.YDDAERR.F K.LVPVGYGIK.R R.FYEQMNGPVAGASR.Q R.RFYEQMNGPVAGASR.Q K.SLAGSSGPAGSSGTSGDHGELVVR.I R.ATAPQTQHVSPMRQVEPPAK.K phosphorylation sur le S M.ATNFLAHEK.I + Acetyl (N-term)	8 31 32 18 16 40 47	8 31 32 18 16 40 47
Bcl-2-associated transcription factor 1(Btf)	T.IAPQNAP.R S.SFYPDGGDQETA.K	30 8	30 8
ATP-dependent DNA helicase 2, subunit 1	K.KPGGFIDSLFYR.D	54	54
<i>Ribonucleoprotein</i>			
Histone-binding protein RBBP7	R.SDSFENPVLQQHFR.N R.ILELDQFKGQQGQKR.F K.IISSDRDLLAVVIFYGTEK.D	37 15 10	37 15 10
Heterogeneous nuclear ribonucleoprotein G	K.TVALWDLR.N + kynurenin (W) K.TVALWDLR.N + DOUBLE Ox (W) R.RLNVWDLSK.I + kynurenin (W) R.YMPQNPQHIAIT.K.T M.ASKEMFEDTVEE.R.V + Acetyl (N-term) K.DYALHWLVLGTHTSDEQNHLVVAR.V + DOUBLE Ox (W) K.IGEEQSAEDAEDGPPELLFIHGGHTAK.I	21 20 40 45 40 25 60	21 20 40 45 40 25 60
Heterogeneous nuclear ribonucleoprotein K	R.NPLPPPPPPR.G R.TDYNASVSPDSSGPER.I	51 51	51 51
40S ribosomal protein S3	R.VTPTRTEIIIATR.T R.FGFPEGSVELYAEK.V R.ELAEDGYSGVEVR.V R.FGFPEGSVELYAEKVATR.G	10 23 8 8	10 23 8 8
<i>Ubiquitination</i>			
26S proteasome non-ATPase regulatory subunit 12	R.VEFILEQMR.L R.LAGIINFQRPK.D R.LQEVIETLLSLEK.Q	12 27 69	12 27 69
Calcyclin-binding protein	K.AELLDNEKPAAVVAPITTGTVK.I K.KAELLDNEKPAAVVAPITTGTVK.I K.IYTLLTGVHQVPTENVQVHFTER.S	21 62 62	21 62 62
Ubiquilin-1	R.ALSNLESIPGGYNALR.R R.FKSHTDQLVLFAGK.I R.ALSNLESIPGGYNALRR.M R.QLIMANPQMQLQIQR.N R.QQLPTFLQQMQNPDTLSAMSNPR.A	32 57 31 0 1	32 57 31 0 1

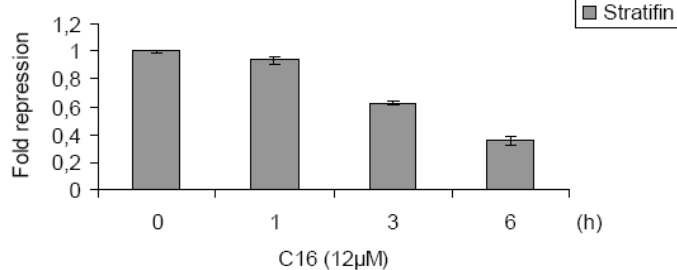
	K.EKEEFAVPENSSVQQFKEEISKR.F	34	
Signaling			
Serine/threonine-protein phosphatase 2A 56 kDa regulatory subunit beta isoform	K.LSTIALALGVER.T K.VLVMANDPNYLHR.M K.SEIVPLFTSLASDEQDSVR.L K.IGPILDNTALQGEVKPVLQK.L R.QISQEHTPVALEAYFVPLVKR.L	19 1 3 47 5	9
Serine/threonine-protein phosphatase 2A 65 kDa regulatory subunit A alpha isoform	K.LSTIALALGVER.T K.KLSTIALALGVER.T R.YMVADKFTELQK.A K.SEIIPMFSNLASDEQDSVR.L K.IGPILDNSTLQSEVKPILEK.L K.VLELDNVKSEIIPMFSNLASDEQDSVR.L	33 28 29 32 84 20	12
	K.LSTIALALGVER.T R.YMVADKFTELQK.A R.LNIISNLDCVNEVIGIR.Q K.SEIIPMFSNLASDEQDSVR.L K.IGPILDNSTLQSEVKPILEK.R R.AISHEHSPSDLEAHFVPLVK.R K.VLELDNVKSEIIPMFSNLASDEQDSVR.L	48 27 24 35 94 74 36	13
	K.LSTIALALGVER.T R.YMVADKFTELQK.A K.IGPILDNSTLQSEVKPILEK.L	21 10 44	14
Ras-GTPase activating protein binding protein 1	K.VLSNRPIMFR.G K.NLPSPGAVPVVTGIPPHVVK.V K.LPNFGFVVFDSEPVQK.V K.NSSVHGGLDSNGKPADAVYGGK.E K.VPASQPRPESKPEQIPPPQRQ.R.D K.SSSPAPADIAQTVQEDLR.T Phospho (STY)	6 63 90 60 8 104	11
Ran-specific GTPase-activating protein	R.FLNAENAQK.F R.FASENDLPEWKER.G + kynurenin (W) R.FASENDLPEWKER.G + DOUBLE Ox (W)	48 26 34	41
Others			
NSFL1 (P97) cofactor (P47)	K.EANLLNAVIVQR.L R.SYQDPSNAQFLESIR.R K.ASSILINESEPTTNIQIR.L	38 32 67	24
Membrane-associated progesterone receptor component 1	K.FYGPEGPYGVFAGR.D R.KFYGPEGPYGVFAGR.D	50 30	42
Annexin A5	K.GLTDEEISLLTSR.S R.SIPAYLAETLYYAMK.G K.WGTDEEKFITIFGTR.S + kynurenin (W) R.GTVTDFPGFDERADAETLR.K	30 12 50 18	35
Actin, cytoplasmic 2	R.GYSFTTAER.E R.AVFPSIVGRPR.H K.QEYDESGPSIVHR.K K.SYELPDGQVITIGNER.F R.VAPEEHPVLLTEAPLNP.K.A	28 23 52 71 78	26
	R.AVFPSIVGRPR.H K.SYELPDGQVITIGNER.F R.VAPEEHPVLLTEAPLNP.K.A	23 39 18	28

Proteins were identified by searching against the NCBI databases using MASCOT (Matrix Science, www.matrixscience.com, London, UK). All searches were carried out using a mass window of 100 ppm and with "Homo sapiens" as taxonomy in NCBI nr database (<http://www.ncbi.nlm.nih.gov>) and 0.5 Da of tolerance on MS/MS fragments. The search parameters allowed fixed modifications for cysteine (carboxyamidomethylation) and methionine (oxidation) and variable modifications on tryptophan (double oxidation or kynurenin) as well as peptide N-terminal E or Q as pyroGlu. Two missed cleavages were allowed.

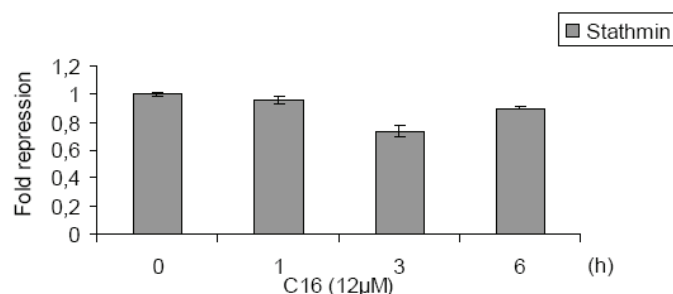
Figure S2. Western blottings were performed in triplicate and analysed by densitometry (Western blots Figures 3, 5 and 6 of the article). The intensity of each band was measured with the Quantity One Software (Biorad, Hercules, CA). To normalize protein levels, the value of the band corresponding to each protein was divided by the intensity of the corresponding α -tubulin band used as internal standard.

Fig. 3

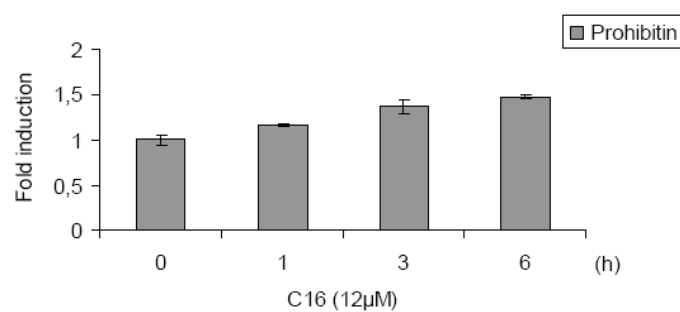
A



B



C



D

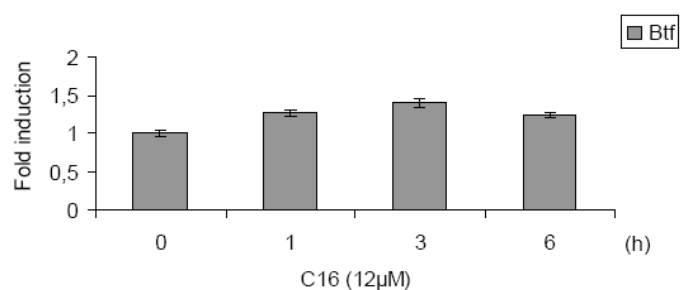


Fig. 5

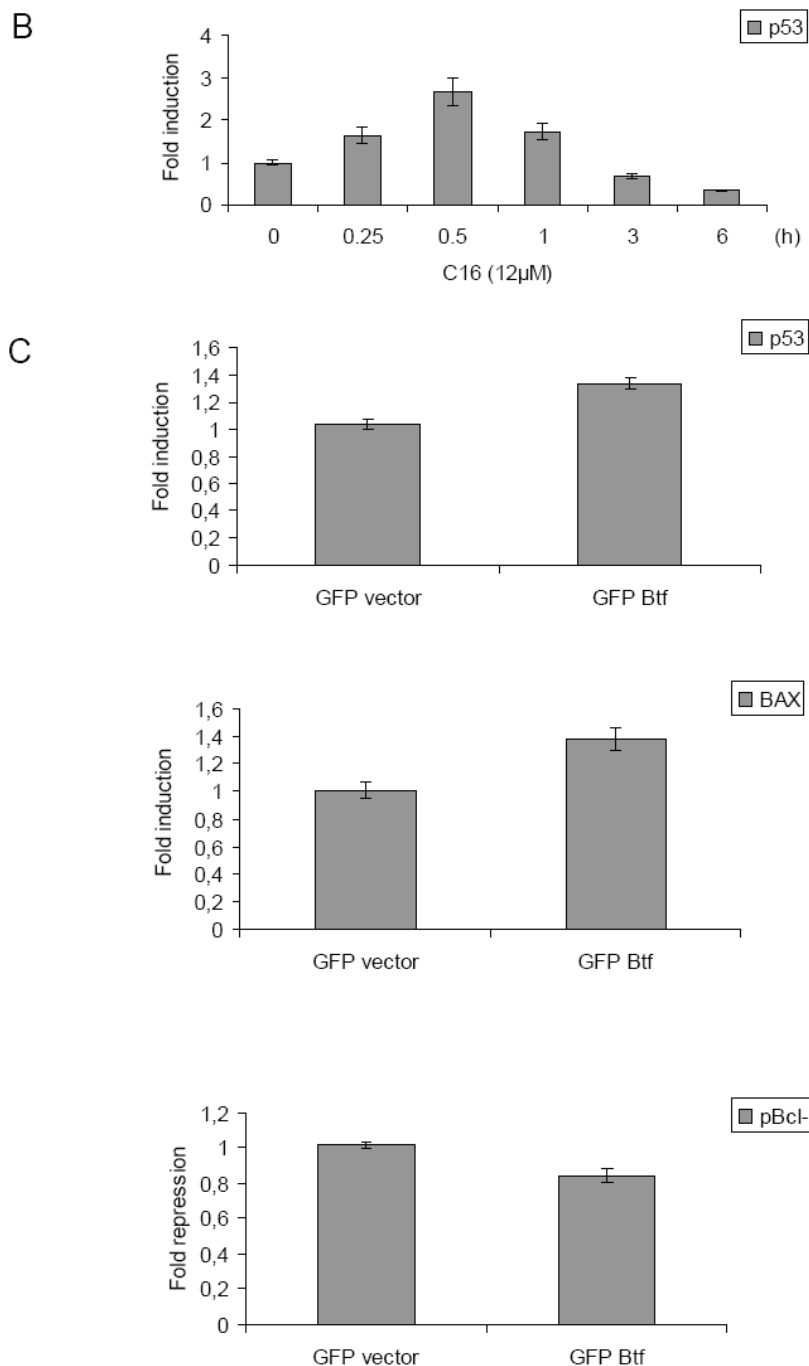


Fig. 6

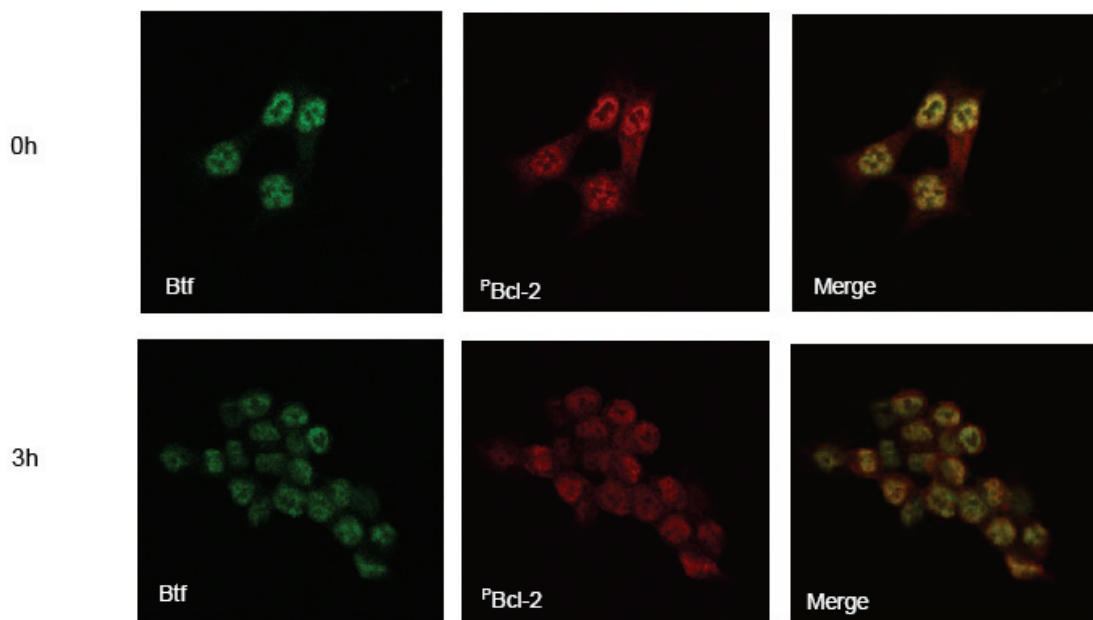
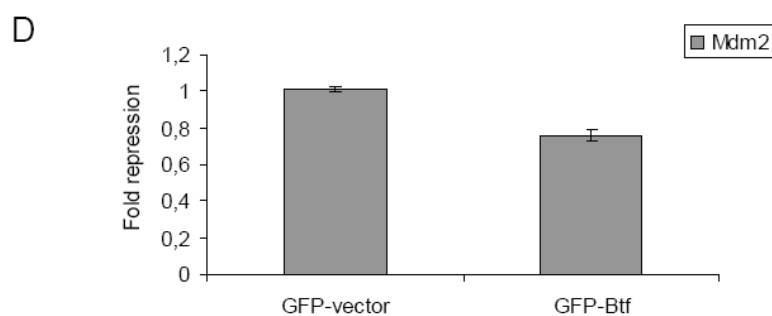
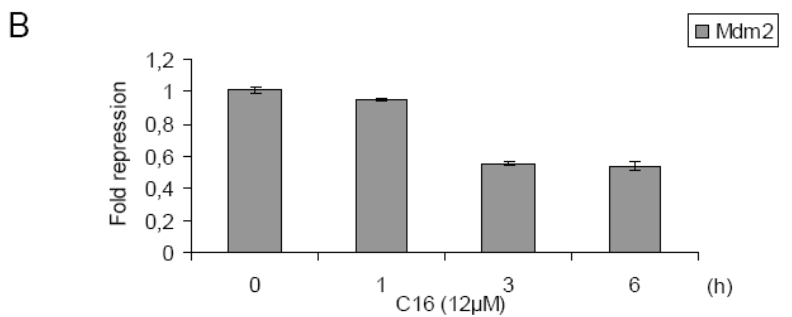


Figure S3. Endogenous Btf is expressed in HCT116 cells and co-localizes with pBcl-2 in the nucleus. HCT116 cells untreated or treated with C16-ceramide during 3 h were stained with both anti-Btf and pBcl-2 antibodies and analysed with confocal microscopy (Leica). The primary antibodies were used as follows: anti-Btf was used in a 1:50 dilution (BD Biosciences Pharmingen, San Diego, CA) and anti-pBcl-2 was used in a 1:50 dilution (Santa Cruz, CA). Bound antibodies were detected by using FITC- or TRITC-conjugated anti-mouse or anti-rabbit secondary antibodies in a 1:500 dilution (Jackson Immunoresearch Laboratories, West Grove, PA).

3. Annexe

Some of the experiments performed in the first part of this work have not all been included in our article in *Journal of Proteome Research*. These results are presented here.

Comparison of the ceramide levels observed in different cell lines

As many studies have shown that exogenous short length ceramides (mainly C2- and C6-ceramides) induce apoptosis, we first investigated which kind of endogenous ceramides are present in four cancer cell lines. Using a previously developed LC-MS-MS method (Fillet *et al.* 2002), C16-, C18-, C20-, C22-, and C24-ceramides were found to be constitutively present in four cell lines (HCT116, MCF7 A/Z, U937 and Ovcar) (Figure A1). Interestingly, short length ceramides (below C16-ceramide) are not constitutively expressed in those cell lines.

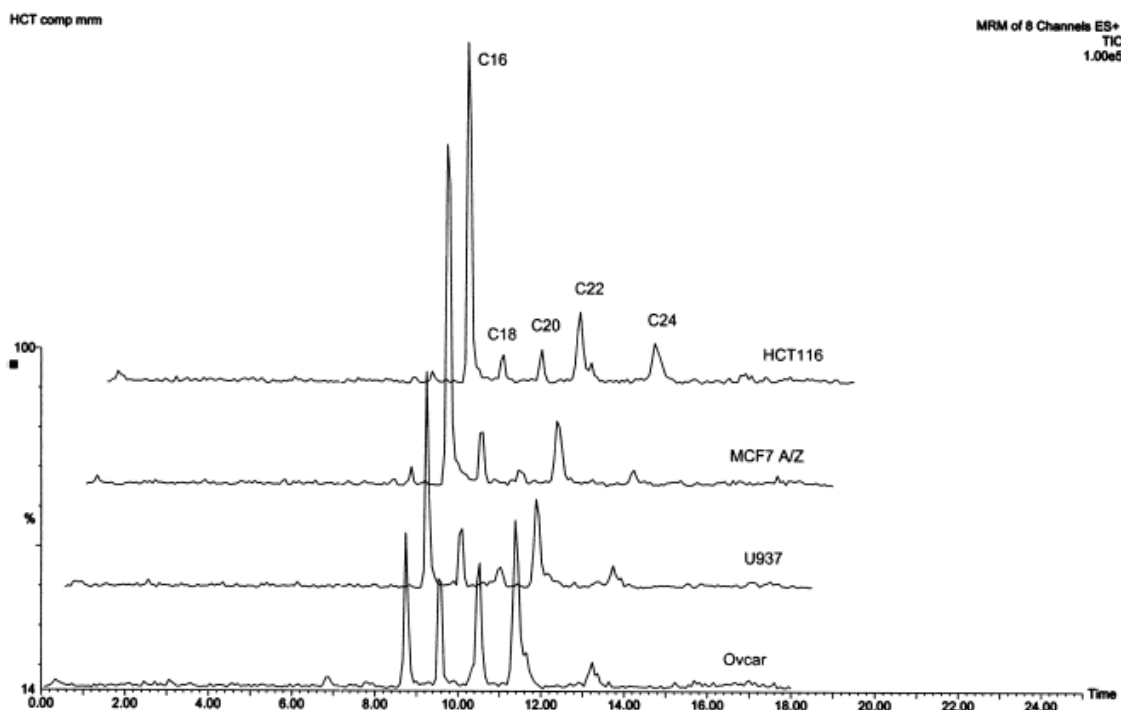


Figure A1. Multiple reaction monitoring (MRM) chromatogram of endogenous ceramides by LC-ESI-MS-MS in four cancer cell lines, HCT116 (colon), MCF7 A/Z (breast), U937 (lymphoid), Ovcar (ovarian). Time scale in minutes (Fillet *et al.* 2002).

We decided to compare C16-ceramide endogenous level in six cell lines in basal conditions: HCT116 and HT-29 (human colon adenocarcinoma cells), COS-1 (immortalized monkey kidney cells), HL-60 (human promyelocytic leukaemia cells), U937 (human lymphoma cells), K562 (human myeloid leukaemia cells). As can be seen in Figure A2, C16-ceramide was at the highest level in the adenocarcinoma cell line HCT116, compared to other cell lines.

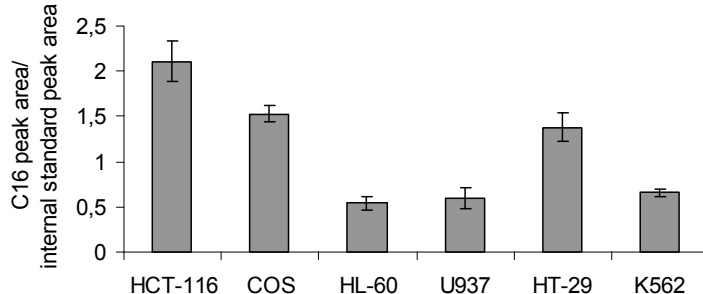


Figure A2. C16-ceramide was detected in different cell lines by reverse-phase chromatography coupled with tandem mass spectrometry (LC-ESI-MS-MS). Cell lysates (corresponding to 500 µg of proteins) of these six cell lines were spiked with a constant amount of internal standard (10 ng of C12-ceramide). The lipid extraction was performed according to the procedure described in Fillet *et al.*, 2002. We calculated a ratio of the peak area of C16-ceramide to that of the internal standard (C12-ceramide).

Then, we measured the endogenous levels of several long chain ceramides species (C14-, C16-, C18-, C20-, and C24-ceramides) in HCT116 cells. As shown in Figure A3, C16- and C24-ceramides appeared to be the predominant subtypes found in HCT116.

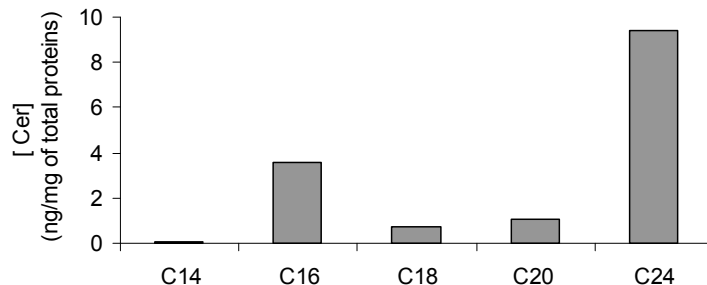


Figure A3. C16- and C24-ceramides appeared to be predominant subtypes found in HCT116. To calculate the concentration of C14-, C16-, C18-, C20-, and C24-ceramides in HCT116 control cells, a calibration curve for each ceramide was established with increasing amounts of each (0.025 ng/µl, 0.05 ng/µl, 0.25 ng/µl, and 0.50 ng/µl). A constant amount of internal standard (10 ng of C12-ceramide) was added to each calibration solution and also to cell lysate corresponding to 500 µg of proteins of untreated HCT116 cells. The lipid extraction was performed according to the procedure described in Fillet *et al.*, 2002. The level of each ceramide was measured by ESI-LC-MS/MS. Result is representative of three independent experiments.

Incorporation of C16-ceramide into HCT116 cells

To mimic the biological effect of endogenous ceramide and because exogenous short-chain ceramide can not mimic endogenous ceramide (van Blitterswijk *et al.* 2003), HCT116 cells were stimulated with exogenous long chain ceramide (C16-ceramide, 12 µM). On the contrary to synthetic short chain ceramide that are water-soluble and membrane-permeable, the extracellular long chain fatty acid ceramide fail to get inside the cell (Ji *et al.* 1995; Fillet *et al.* 2003; van Blitterswijk *et al.* 2003).

However, Ji and its collaborators found that a solvent mixture consisting of ethanol and dodecane (2% v/v) could solubilize ceramide and help the dispersion of natural bovine brain ceramide that they used, into aqueous solution (Ji *et al.* 1995). Therefore, this strategy was adapted and tested in our model of colon cancer cell line. Briefly, C16-ceramide was dissolved in ethanol at 37 °C. Then, dodecane (0.02% of culture medium volume) was added to the ethanolic solution, mixed and incorporated in the culture medium. It is noteworthy that for all following experiments, an equal amount of solvent (ethanol/dodecane) was added to control cultures (untreated cells) compared to the corresponding ceramide treated conditions.

To examine whether this vehicle (dodecane) can deliver exogenous chain C16-ceramide into cells, we verified the cellular incorporation of this ceramide in HCT116 cells by tandem mass spectrometry. A 2-fold increase of C16-ceramide cell content was measured by mass spectrometry after 15 min of cell contact (data not shown).

Btf isoforms and localization

In the present study, Btf was found, for the first time, to be implicated in the apoptotic signal triggered by ceramide. This protein was found to be upstream of well-known apoptosis-related proteins such as Mdm2, BAX and Bcl-2 (Renert *et al.* 2009).

Moreover, four isoforms produced by alternative splicing have been described for Btf (isoform 1, 106 kDa; isoform 2, also known as Btf_L, 105 kDa; isoform 3 also known as Btf_S, 100 kDa; isoform 4, 86 kDa) (from Protein knowledgebase, UniProt KB, Expasy Proteomics Server, accession no.Q9NYF8). Kasof *et al.* described the function of Btf_S, which differs from Btf_L in 49 amino acids in the C-terminal region (Kasof *et al.* 1999).

We checked whether all Btf isoforms expression is modified in response to C16-ceramide treatment (Figure A4). We observed that the expression of the different known isoforms of Btf was increased in a time-dependent manner after C16-ceramide treatment. However, as shown in Figure A4, the antibody recognized a band in the nuclear fraction of HCT116 cells, with a mass of approximatively 150 kDa. This is consistent with that reported by Haraguchi *et al.* (Haraguchi *et al.* 2004). Moreover, this band seemed to be specific, because like all the bands corresponding to different known isoforms, it disappeared after a Btf siRNA transfection. The same Btf band was observed in total extracts of HCT116 cells (Renert *et al.* 2009).

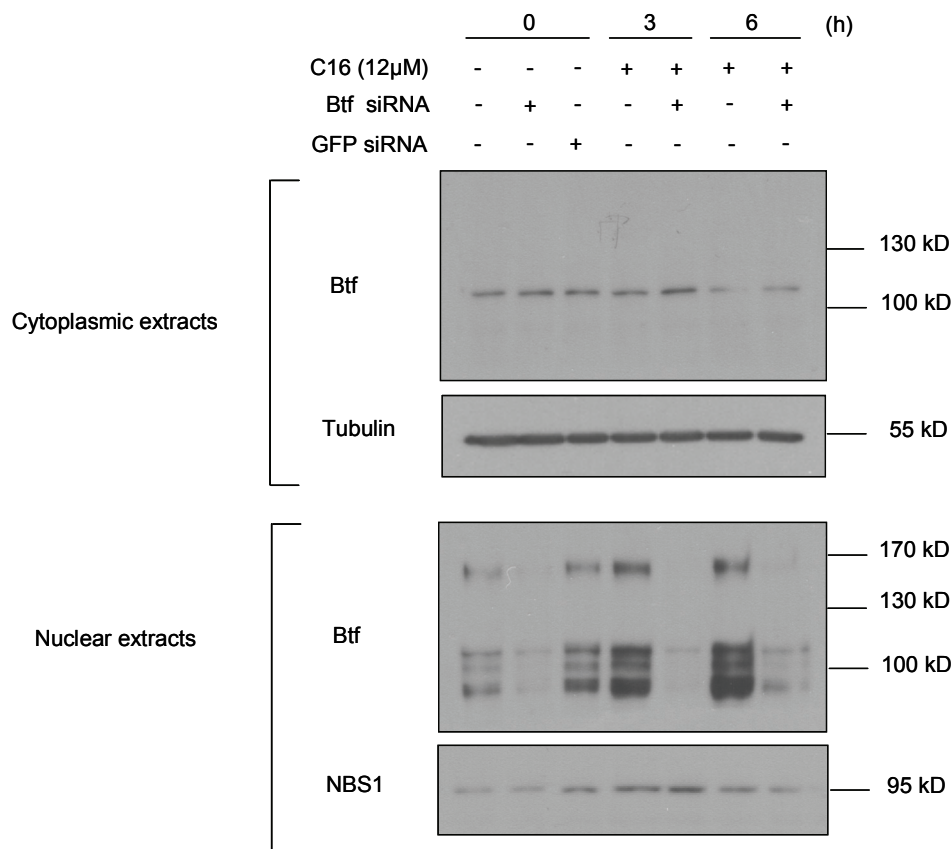


Figure A4. Btf expression is increased after C16-ceramide treatment. HCT116 cells were transfected with GFPsiRNA or Btf siRNA and subsequently left untreated or stimulated with C16-ceramide for 3 and 6 h. Cytoplasmic and nuclear extracts were separated on SDS-polyacrylamide gels, and immunoblotting was revealed with anti-Btf, -NBS1, and α -tubulin antibodies.

De novo generated ceramide and exogenous C6-ceramide have been shown to regulate the alternative splicing of caspases-9 and Bcl-x pre-mRNA. This mechanism has been shown to be mediated by protein phosphatase 1 (PP1) (Pettus *et al.* 2002). Previously, the dephosphorylation of SR proteins in response to the *de novo* generation of endogenous ceramide was found to be dependent on PP1, a ceramide activated protein phosphatase (Chalfant *et al.* 2001).

Therefore, to establish whether a ceramide-activated protein phosphatase (CAPP) played a role in regulating the Btf expression, we first pretreated HCT116 for 2 h with 25 nM calyculin A, an inhibitor of both PP1 and PP2A. Secondly, HCT116 cells were pretreated for 2 h with 10 nM okadaic acid, a selective PP2A inhibitor (Lee *et al.* 1996; Chalfant *et al.* 2001; Pettus *et al.* 2002) (Figure A5). We observed that calyculin A, but not okadaic acid, inhibited the increase of Btf isoforms expression levels mediated by ceramide treatment (Figure A5). These results suggest that PP1 could mediate the C16-ceramide effect on the expression levels of Btf isoforms.

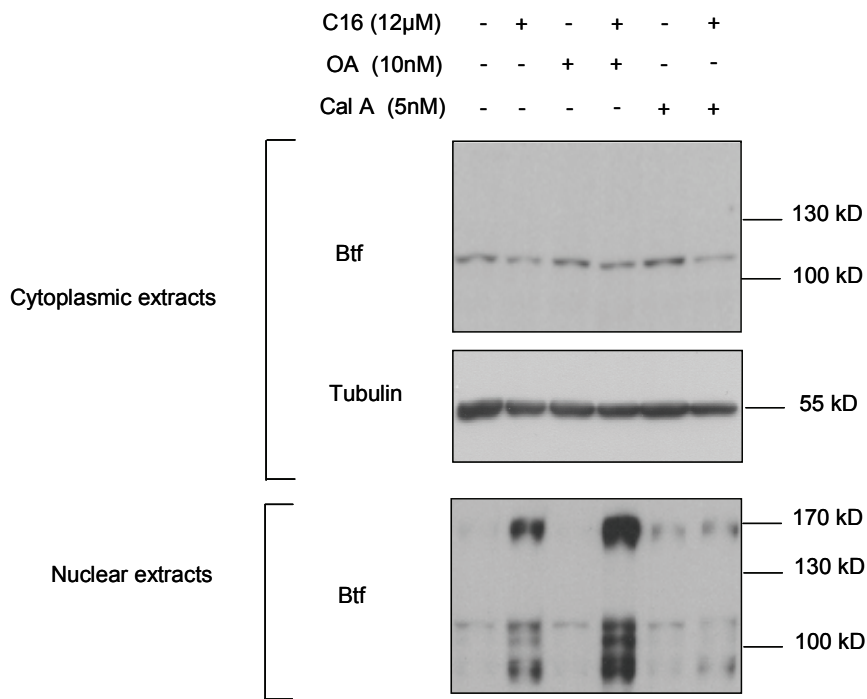


Figure A5. Effects of inhibitors of serine/threonine protein phosphatases, PP1 and PP2A. HCT116 cells pretreated 2 h with either 10 nM okadaic acid or 25 nM calyculin A followed or not by 6 h treatment with 12 μ M C16-ceramide. Cytoplasmic and nuclear extracts were subjected to anti-Btf and α -tubulin antibodies for Western blot analysis. Data are representative of three independent experiments.

4. Conclusion

In this first part of our work, we showed that exogenously-supplied natural long chain ceramide (C16-ceramide) induced a decrease in viability of adenocarcinoma cells (HCT116), partly due to apoptosis. Using 2D-DIGE approach, we then identified new proteins involved in the apoptotic pathway triggered by exogenous C16-ceramide. Especially, we found that ceramide up-regulated Btf, a transcriptional repressor. Furthermore, we have identified a new signalling pathway specifically induced by C16-ceramide, depending on Btf and leading to down-regulation of the Mdm2 protein expression. We have not yet determined the link between ceramide and Btf. Nevertheless, this study constitutes the first demonstration of an implication of the death promoting factor, Btf, in the proapoptotic ceramide dependent signalling pathway.

